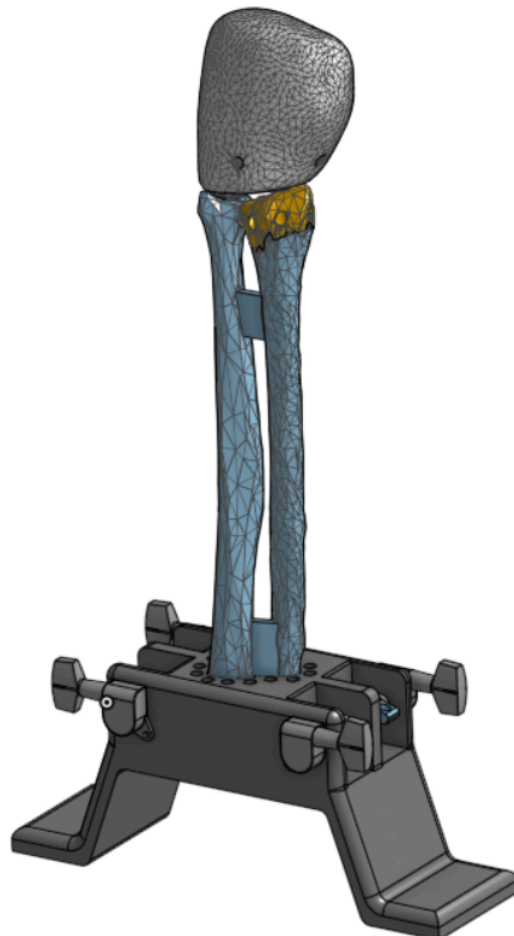# Designing an Affordable Distal Radius Fracture Reduction Simulator for Medical Training

Natalie Bretton, Ryan DeLoach, Lauren Elliff, Brian Garmer, Greer Matthias, John Murphy,

Katya Napolitano, & Ethan Norris

4/29/2025

Project Advisor - Jason Forman

Problem Statement

A Distal Radius Fracture (DRF) is one of the most common types of wrist fractures, with more than 640,000 DRFs occurring in the United States in 2001 (Chung & Spilson, 2001). This type of fracture occurs when the long bone on the thumb side of the forearm fractures close to the wrist. Often, the broken fragment displaces as it has various tendons and muscles that exert tensile force on it. Before a cast or splint can be applied to a fractured wrist, the misaligned, fractured bone must be manually put back into place to prevent improper healing of the bone. In the case of DRFs, the most common practice for this realignment is called closed reduction. This process involves a doctor manually resetting the fracture into its proper configuration by externally manipulating a patient's wrist and musculature. The traditional method for learning how to perform manual reduction has been to practice the procedure on injured DRF patients while under the supervision of experienced professionals (Jackson et al., 2020). While in recent years, a handful of DRF reduction training devices have been developed, they are not widespread in the industry. Generally, the devices are either very expensive or are not optimally designed for the goal of efficient and accurate training. This lack of prevalence is troubling, especially given that studies show the use of training devices leads to better results in manual reduction performance (Jackson et al., 2020). The medical industry would benefit from improved educational simulation technology designed with the intent of accurately simulating the physical feel of performing a closed reduction.

The goal of our capstone project is to create a DRF training device that will be affordable and realistic, hopefully making simulator training devices like ours more prevalent in the medical industry. This will assist doctors in learning closed reduction by creating a controlled environment to effectively master the skill before performing it on patients.

Research

Our design process began with each team member conducting significant preliminary research. Given that our team is composed solely of mechanical engineering students, we had little to no knowledge of the specific physiology surrounding DRF fractures. Accordingly, our research included reading journals and articles on DRF and looking at videos and diagrams of how doctors perform manual reduction. This research period culminated in a meeting with both of our advisors to discuss what we'd learned and receive input. Specifically, Dr. Freilich, a surgeon at the UVA Department of Orthopaedic Surgery, advised us on what specific factors we should focus on to create a design that would accurately mimic a wrist reduction.

Our research also resulted in the discovery that there are a handful of commercially sold products on the market today that seek to solve this problem. However, these products are few and far between, and the existing technologies can cost upwards of $2000 (shown in Figure 1). Additionally, some of the more popular devices are designed for a 6'2" male, which is not representative of the general population that experiences DRF (GTSimulators, 2024). Distal radius fracture is seen across all age groups, with recreational and athletic activities being a major cause of fracture in younger demographics and falls causing many fractures in the elderly population, especially those with osteoporosis. To address some of the areas of improvement for current DRF simulators, we aim to make our device affordable, scalable, and versatile so that it can represent many different patients.
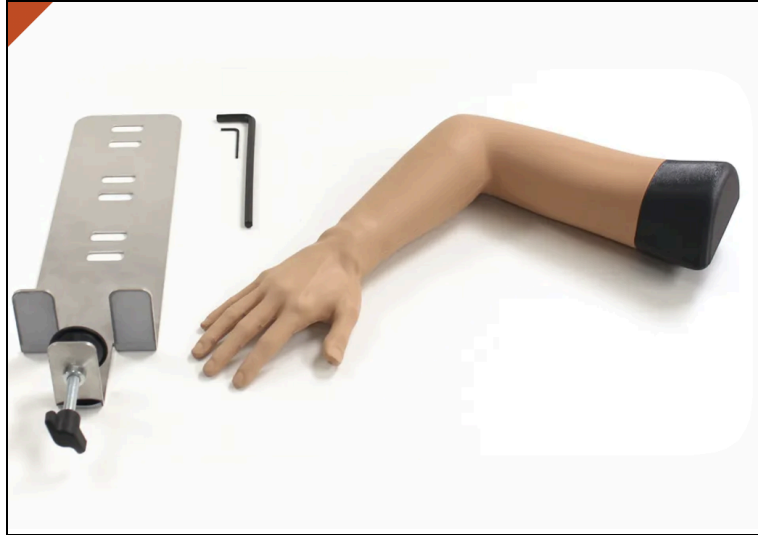
Figure 1
Colles' Fracture Reduction Trainer, Limbs and Things, $2670

In addition to commercially sold products, there are a few other similar technologies that have been developed but not marketed. Dixon et al. (2020) detail a simulator that they developed using 3D-printed bones, a wooden block as a hand, and O-rings for elasticity between the fracture pieces (Figure 2). This model gave us inspiration for some of the techniques that are utilized in our simulator. While we are also 3D printing scanned bones, we do this intending to keep the model scalable. Additionally, 3D printing will allow us to add more detail to the hand portion of the model as compared to a wooden block. Also, the previous device did not mention a way to adjust the tensile force that the tendons and muscles of the forearm exert on the bone fragment. Keeping this force variable and adjustable is one of the main improvements we hope to make with our model. Although this device is not commercially sold, it helped us conceptualize a lot about the design of our model, and we hope to make additions that can improve DRF simulation as a whole.

Figure 2
Existing 3D printed DRF simulator (Figure source: Dixon et al. (2020))

Our advisors, Dr. Forman and Dr. Freilich, also collaborated on a similar mechanism several years ago that produced some research literature, but never made it past the prototype phase. Working in collaboration with them, we were able to discuss some of the areas of improvement that they identified from their design process. Another area of research that we looked into was how we could mold a hand to create an outer layer of silicone flesh for the device. Powell et al. (2019) used a 3D-printed system of molds to design a high-fidelity facial flap for practicing plastic surgery. This method used negative and positive molding to make a

thin layer of silicone that has a similar texture to human skin, which is one of our requirements. We are taking inspiration from this method of molding as our model also has to be realistic, and by 3D printing the molds we can easily adjust the model to represent people of various anthropometries.
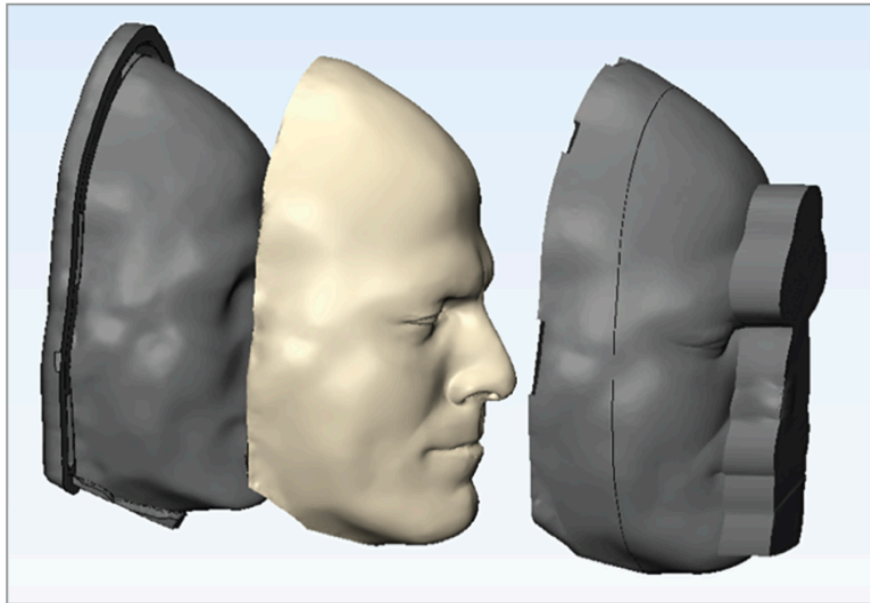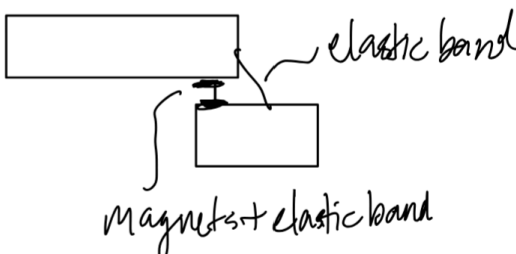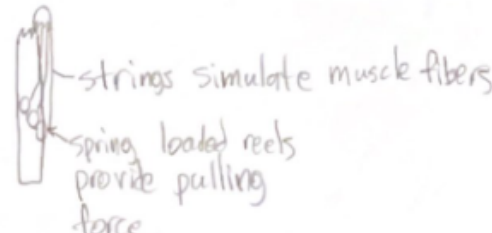

Figure 3
CAD representation of the Facial Flap Simulator Manufacturing Assembly (Figure Source: Powell et al., (2019))

Many previous papers helped us learn about the benefits of medical simulations and various possible design methods for our device. The few we mentioned are the projects that have contributed to the design of our model the most. This background research contributed both anatomical knowledge of the wrist and previous design ideas for our first round of ideation.
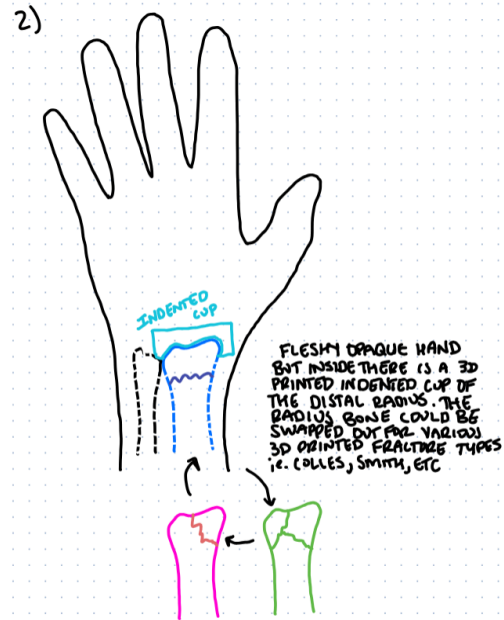
Ideation

To begin our ideation process, each member of our team created a series of ideas to bring to the whole team. Each group member presented the idea that they thought was best, and those ideas are shown in Table I below. With these ideas, we moved forward with screening and selection.

Table I
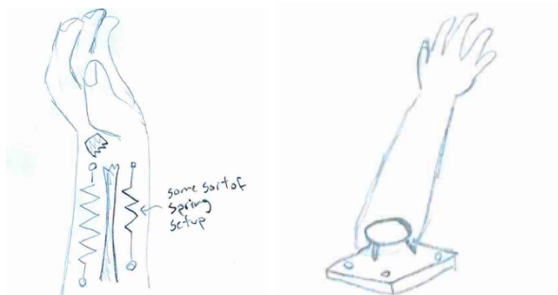Ideas Presented after First Round of Ideation

A	B
Elastic bands to hold the "bones" together and represent the tendons. Magnet to represent the initial force required to begin the reduction process.	Strings act like muscle fibers keeping bone out of place, spring loaded reels (like a tape measure) pull the strings in.
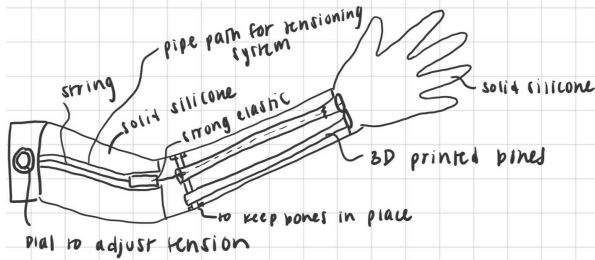
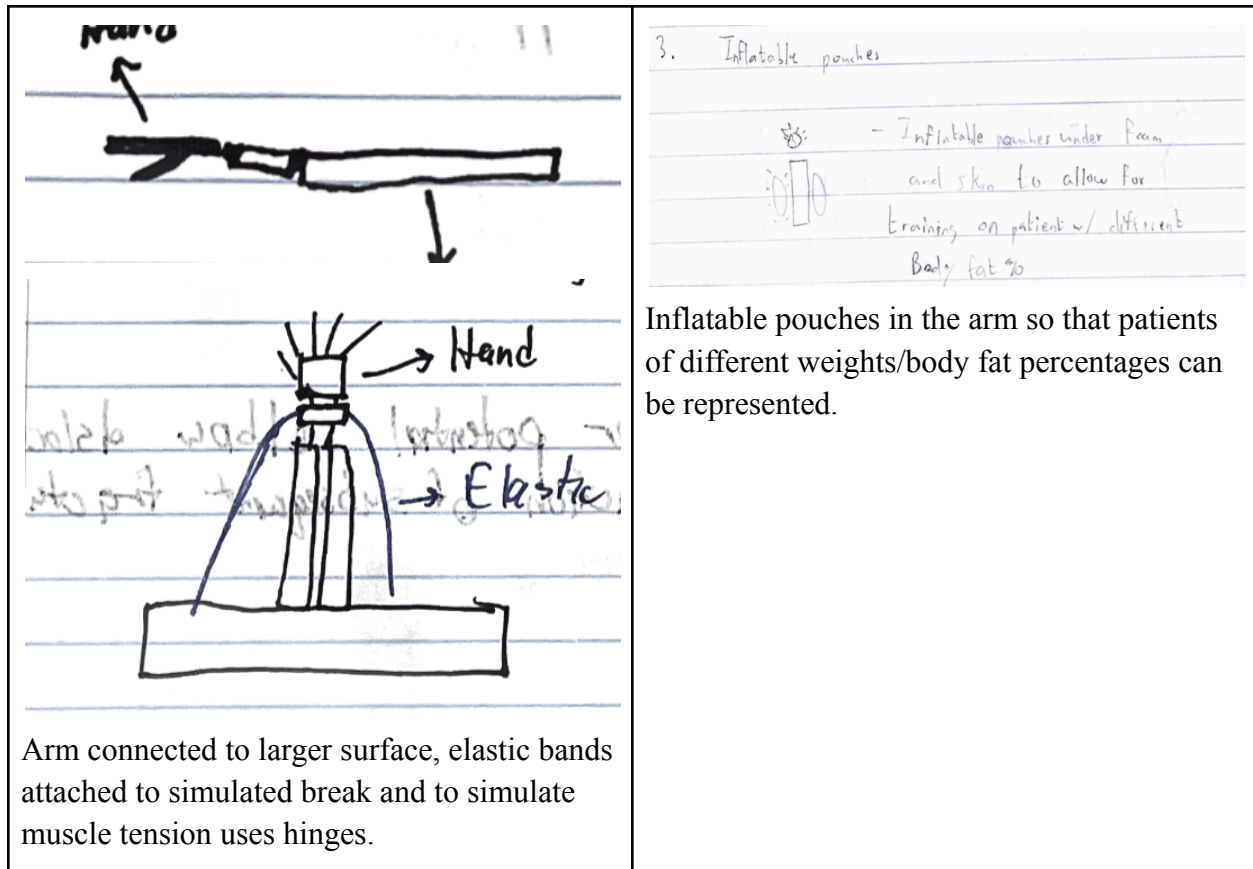| C	D
Realistic silicone model of arm containing elastics within 3D printed bones. Elastics can be tightened and loosened using a dial at the "shoulder".	Indented cup to hold the fractured piece of the radius so that various fracture patterns can be inserted.
E Arm with spring system to represent muscles in tension, mount to limit movement, and mechatronic system to let the user know when the fracture is in the correct position.	**F** Components are snapped into a socket via a tolerance fit. To detach the tolerance fit, the correct motion is needed to replicate reduction. Once detached from the "fracture" position, it is forced into the correct position.
G	**H**

Arm connected to larger surface, elastic bands attached to simulated break and to simulate muscle tension uses hinges.

Inflatable pouches in the arm so that patients of different weights/body fat percentages can be represented.

Selection and Screening

With the design ideas from our ideation process, we created criteria to screen our ideas. Our criteria ultimately came from the main requirements for our training device. The most important requirements relate to the simulator's life-like appearance, including making it anatomically correct, having a flesh-like feel, and requiring the correct motion to reduce the fracture. The other major requirements are that the simulator is low-cost and easily manufactured. These requirements helped create our final list of selection criteria: Anatomically correct, flesh-like feel, easily reproduced, adjustable force, dual equilibrium, realistic reduction,

maintainability, and durability. With these criteria, we compared each idea with idea H to determine if it would perform better (+), worse (-), or the same (0).
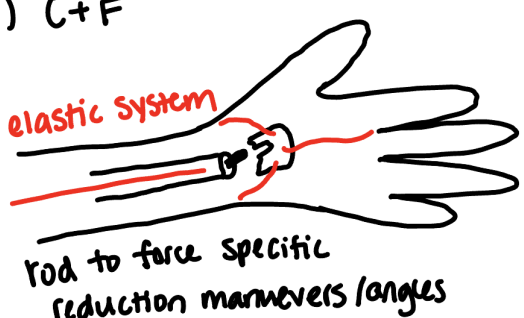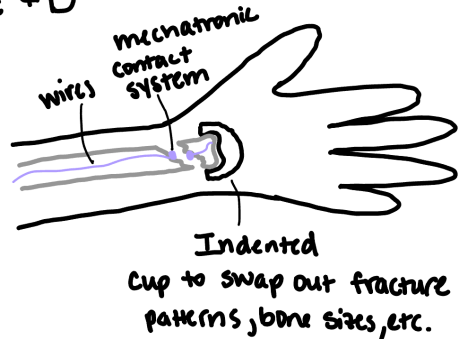
Table II
Screening Chart

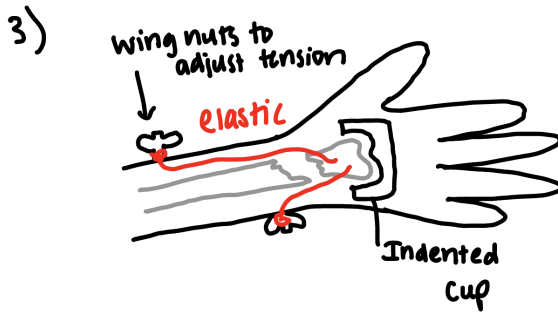|	A	B	C	D	E	F	G	H
Anatomically Correct[1]	0	0	+	+	0	0	–	0
Flesh-like feel[2]	–	0	+	+	+	+	0	0
Easily Reproduced[3]	+	0	–	+	–	0	+	0
Adjustable Force[4]	–	+	+	–	0	0	+	0
Dual Equilibrium[5]	–	–	–	0	0	+	+	0
Realistic Reduction[6]	–	+	0	0	+	0	–	0
Maintainability[7]	+	0	+	+	–	0	+	0
Durability[8]	+	0	+	0	+	+	–	0
+'s	3	2	5	4	3	3	4	0
-'s	4	1	2	1	2	0	3	0
Net Score	-1	1	3	3	1	3	1	0
Rank	8	6	**1**	**2**	5	**3**	4	7

From Table II we chose features of the best designs and combined them to create five new designs stemming from those original ones. These new ideas are listed as Final Ideas 1-5 in

Table III below. We then scored these ideas on a scale of 1 to 5 for each selection criterion. We also weighted the criteria based on which requirements were explicitly stated as important in the project description and which would be most important in the prototyping stage. For example, the criterion with the highest weight was 'realistic reduction' and one of the lower-weighted ones was 'anatomically correct'. We made this decision because we decided that it was more important for the feel of the procedure to be accurate than the anatomy. If getting an accurate reduction motion meant we had to put a force in a direction where a tendon might not be anatomically, then that was alright. We also weighted adjustable force pretty highly as this is what allows our device to represent many different people and not just one type of patient. Other important criteria included durability so the device can be used repeatedly for training, and easily reproduced so that the model can reach many institutions.

Table III
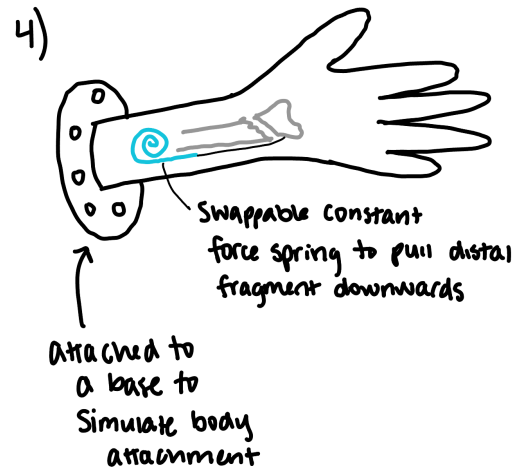Ideas from Second Round of Ideation

Final Idea 1	Final Idea 2
Combination of earlier designs with an elastic system to represent tendons. Rod/pin in the radius so that reduction must be placed in the exact right spot in order to hold.	Combination of earlier designs resulting in a mechanical contact signaling system and an indented cup to represent different fracture patterns.

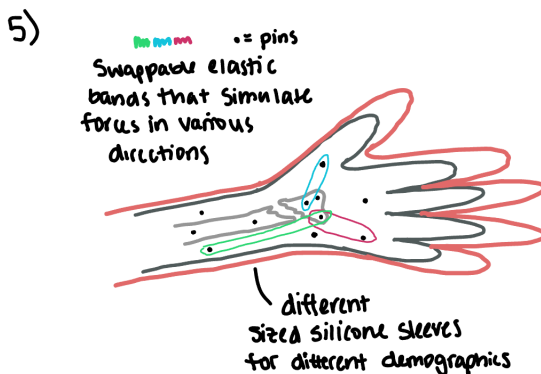| Final Idea 3	Final Idea 4
3) wing nuts to adjust tension elastic Indented cup Combination of earlier designs. Indented cup to allow for fracture pattern swaps and wing nuts to allow for tension adjustment of the elastic.	4) Swappable constant force spring to pull distal fragment downwards Attached to a base to Simulate body attachment Combination of earlier designs. Attached to a base to simulate attachment to the body, an interchangeable spring that pulls the radius fragment down towards the elbow.

Final Idea 5

5) •= pins Swappable elastic bands that Simulate forces in various directions different Sized silicone sleeves for different demographics

Interchangeable elastic bands/pins to change arrangement and force of the forces. Compatible with silicone sleeves to represent different body fat percentages.

Table IV
Scoring Chart

	Wt	1	1-Wt	2	2-Wt	3	3-Wt	4	4-Wt	5	5-Wt
Anatomically Correct[1]	5	3	3	5	5	5	5	4	4	5	5
Flesh-like feel[2]	10	4	8	4	8	4	8	4	8	5	10
Easily Reproduced[3]	15	3	9	2	6	2	6	3	9	1	3
Adjustable Force[4]	15	0	0	0	0	4	12	2	6	3	9
Dual Equilibrium[5]	10	4	8	3	6	5	10	2	4	4	8
Realistic Reduction[6]	25	3	15	2	10	5	25	2	10	4	20
Maintainability[7]	5	4	4	2	2	5	5	3	3	2	2
Durability[8]	15	2	6	3	9	3	9	3	9	2	6
Score	100	23	**53**	21	**46**	33	**80**	23	**53**	26	**63**
Rank			**3**		**5**		**1**		**3**		**2**

From this scoring chart (Table IV), we were able to select an idea to move forward with in design, which ultimately ended up being Final Idea 3.

Initial Specifications

Initial specifications for our reduction simulator included closely replicating the physical feel, look, and weight of a typical arm. The forces required to perform a successful wrist fracture

on the simulator should replicate procedures that would be used on a patient. The simulator must reach static equilibrium in both 'broken' and 'set' positions, and the force required to "set" the wrist must be variable (i.e., there is a mechanism to alter tensions). In order to make this simulator affordable and easily reproducible, the total cost should be less than $150, and a 3D printer should be used along with other widely available materials. Using these initial requirements and constraints, we drafted a list of 21 important specifications outlined in the table below.

Table V
Initial Specifications for Wrist Fracture Reduction Simulator

Specification	Description	Metric
Skin Feel	The "skin" of the simulator must feel realistic enough to allow for accurate training (grippy enough, but pliable)	Subjective tests by engineers and physicians
Skin Elasticity	The "skin" must stretch and bend similar to human skin	Percent elongation and modulus of elasticity testing
Skin Durability	The "skin" should be durable and last through many uses of the simulator	Count number of cycles at greater than expected stress
Cost of Production	Summed cost of producing/ordering must be less than or equal to $150.	Cost in US Dollars
Force Variation	Force required to "set" wrist must be variable (i.e. tensions in soft tissue)	Run tests with different desired forces and ensure that the force required to move the simulator varies
Accessibility of Materials	All materials must be available to a common person	List of retailers that materials can be purchased from by average person

Ease of Construction	Simulator must be able to be constructed with a set of instructions once all materials are gathered	Give instructions and materials to random participants and measure the success rate
Accurate Bone Orientation	Initial position of "bones" must be accurate to a typical distal radius fracture	Comparing physical simulator to x-ray image of distal radius fracture and physician feel
Realistic Fracture Reduction Force	Bones should only be able to move from a "stable" to "unstable" after minimum precise force is applied	Force required to "set" fracture
Replicable	Design ensures every simulator made will be nearly identical	Meeting specifications on multiple models
Resettable Configuration	Must be able to reset the simulator after performing the reduction	Perform cycle testing to make sure the simulator can be reset to the original position without breaking or losing stiffness
Ability to Calibrate	Can measure and indicate the amount of force necessary for different variations of fracture reduction and variable forces required	Use force gauge to record required force for each calibration and compare it to simulators reading
Easily Adaptable for Different Fracture Types	Simulator can be modified with minimal effort to simulate different types of fractures	Number of different fractures it could be potentially compatible with and how many steps swapping the model takes
Physical Verification	Ability to physically verify that the fracture reduction was performed correctly	Indication of successful reduction exists and is corroborated by trained physician
Ability to Splint or Cast	The simulator must be able to	Setting and removing a cast

	have a splint or cast applied to it by students	and ensuring there is no damage to simulator
Weight	The simulator must weigh a similar amount to the limb of a similar size	Measure weight with scale
Scalable Simulator	The simulator can be easily scaled to create smaller or larger models to accurately simulate different sized people	Measure the components of each sized simulator and compare it to anatomical data of the corresponding demographic of people
Two Equilibriums	Has to reach a static equilibrium in both 'broken' and 'set' positions	Test both broken and set positions to ensure the device is stable and will not deviate from equilibrium with minimal forces
Accurate Reduction Motion	The motion required to use the simulator is the same as seen in real patients	Physician feel
Compatible with Current Technology	Should work with splints, finger traps, etc.	Get physician to try some of their current methods out with the simulator and measure the success rate
Interchangeable Components	Ease of swapping specific parts such as bones or mechanical components to ensure easy repair	"Break" the simulator and measure the ease and amount of parts to fix it

Our initial prototype can be seen in Figure 4. Material choices in the design were made with the goal of accessibility. The main structure was the bone, base plate, and fracture which were 3D printed using PLA to ensure the product is accessible and cost-effective, while also providing the necessary strength for our goal. To avoid deformation in the bones and attachment

15

blocks, we made sure that the stress in those components did not exceed the yield strength of PLA plastic, around 48 MPa. With regard to the marginal value, we want to ideally minimize the amount of elastic bands that we need to use. In our initial prototype we had four elastic bands, two running up the dorsal (backside) of the hand and two running up the ventral (frontside). Components of our initial design were intended to provide variability in our first prototype. Features such as the various holes in the base and in the radius allowed us to change the location of our elastic bands and therefore adjust the direction of the forces. Furthermore, we were able to vary the tension in our band by pulling it tighter or looser and pinning it at the base of the model. Both of these design choices alter the physical feel of the simulator, allowing us to make frequent alterations to accurately capture the motion and feel of reduction. This variability was important for testing with Dr. Frelich as we were able to make adjustments to the path and amount of tension in accordance with his advice to provide an accurate feel of reduction.

The second iteration saw minor improvements to the location of holes in the base and better resolution holes in the fracture pattern. The third iteration saw more extreme changes to improve the accuracy of the model, implement a way to alter the tension of the elastic bands, and provide the capability to apply a splint after the reduction had been performed. The accuracy was improved by making concrete decisions on the path of the elasticity under guidance from Dr. Frelich and a more accurate hand model was implemented. Furthermore, mechanical stops were added to the hand via zip ties to ensure the motion was not unrealistic and could stretch indefinitely. The base was altered by having an open portion with stands on each side. This allowed the model to be clamped to a surface such as a table and the open portion allowed space for a splint to be wrapped around and attached to the hand to stabilize the fracture after the

reduction. Lastly, a mechanism to alter the tension was implemented in the base by having pegs that could be rotated with guitar tuners to tighten or loosen the elastic.

Preliminary Analysis

Figure 4

Final CAD model of our initial prototype. Pictured are the base block (blue), bones (tan), hand block (grey), and elastics (yellow and blue).

A CAD model of the inner components of our design (bones, elastics, base and hand blocks) was developed using Onshape, a collaborative 3D modeling software. STL files of the radius and ulna bones were downloaded from Thingiverse, a website containing a vast collection of STL files available for free download and use. After correctly orienting the radius and ulna

bones, we designed the base and hand blocks. We made sure the blocks would provide a sufficient amount of space for the attachment of the bones while maintaining roughly similar dimensions to that of the upper forearm and wrist. The hand block was rounded and smoothed to mimic the slender shape of the hand and to prevent any rough edges from ripping the silicone skin. Holes were added to various positions along the bones and base block to allow for a range of elastic attachment configurations.
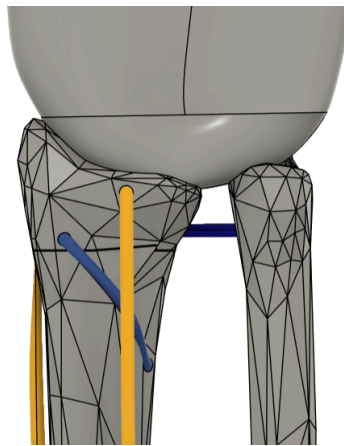

Figure 5
Tendons that stabilize and connect the wrist and forearm are represented by silicone elastics, colored blue and yellow for visibility.

In our model, three main elastics were positioned to represent the major tendons applying forces to the bones. The radioulnar ligaments connect the proximal segments of the radius and ulna, and the triangular fibrocartilage complex and interosseous membrane were included because they stabilize the radioulnar joint and forearm, respectively. To allow for a "broken" equilibrium position, a fourth elastic was incorporated to connect the broken segment of the radius to the main body of the bone. This ensures that we can control the path that the bone takes once it is "broken".
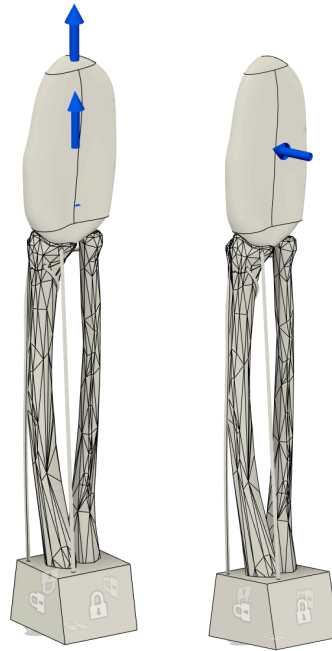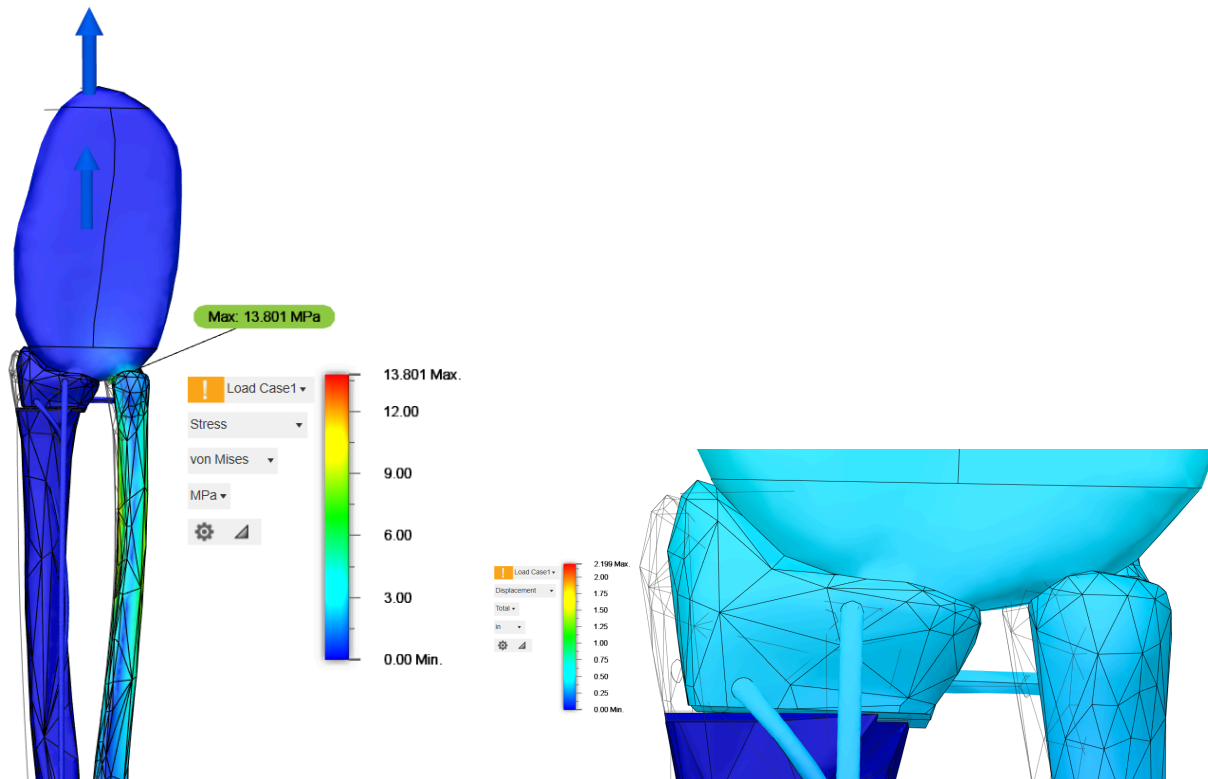
Figure 6
Simulation setups for wrist fracture reduction assembly

Finite Element Analysis (FEA) was performed on the final assembly of our CAD design

in order to verify that our system can correctly respond to the various forces that result from a

manual reduction, as well as determining any weak points in our design. A static simulation in

Fusion360 was performed to achieve this. To allow for easier computing, the assembly was

simplified by removing unnecessary holes and fillets. ABS (acrylonitrile butadiene styrene)

plastic, which is widely available and affordable, was selected for the attachment blocks and

bones of our design. It was chosen due to its high durability and tensile strength; applicable in

our design since the reduction procedure requires a large amount of pulling on the hand and

bones. Silicone was selected for the elastics, but the exact type of elastic we will use in our final

design may be changed later in the prototyping and testing process. The body was constrained in

all directions on the base block, and contact bonds were applied to all attachment sites. 25 pound

horizontal and vertical loads were distributed evenly along the outer surface area of the hand block. 25 pounds of force was selected since it is larger than the amount of force applied in a manual reduction, and results would indicate how our design would react to extreme force scenarios.

Figures 7 and 8

FEA results for the stress (Figure 7) and displacement (Figure 8) of our design under a 25 lb vertical force. A maximum stress of 13.8 MPa occurs in the attachment region between the ulna and the hand block. The displacement results show that the broken portion of the radius displaces upwards and to the right relative to the constrained body.
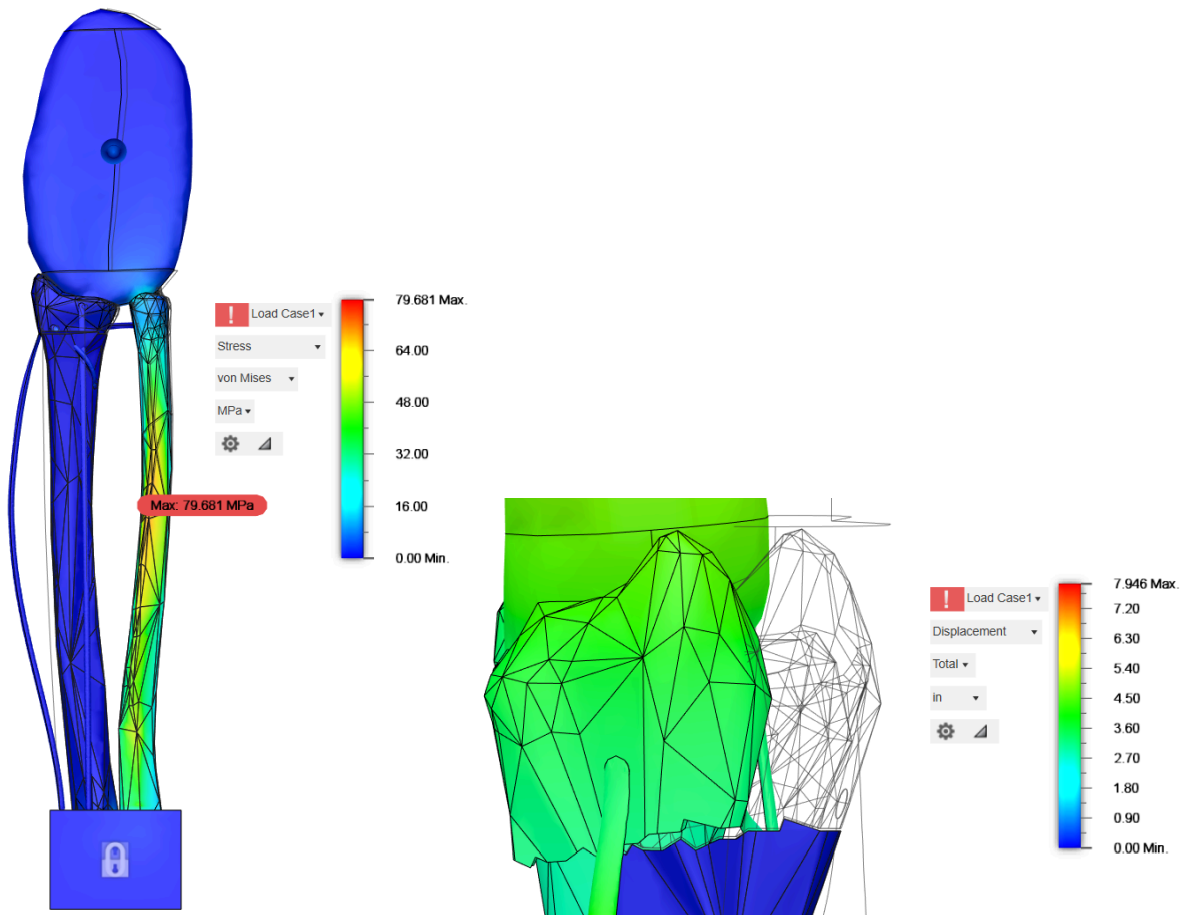
Figures 9 and 10
FEA results for the stress (Figure 9, front view) and displacement (Figure 10, side view) of our design under a 25 lb horizontal force. A maximum stress of 79.68 MPa occurs in the center of the ulna. The broken segment of the radius has a large displacement of roughly 5 inches (generated model is not to scale).

Final results show that the simulator correctly responds to the different applied forces, with the proximal broken segment of the radius moving in the correct horizontal and vertical directions. Results also suggest that the ulna is highly likely to deform under large horizontal forces. The central portion of the ulna experiences a stress of about 80 MPa, which is much larger than the yield strength of ABS plastic (~48 MPa). To mitigate this, we will need to increase the infill pattern and percentage around this weak point of the ulna. It is important to

note that such a large horizontal force would not be applied in a regular reduction procedure; the largest force results from the vertical pulling of the hand, which our design can withstand.

In addition to the FEA analysis used to validate the mechanics of the model, calculations were done on the elastic tightening mechanism that represents the variable muscle/tendon force present in the forearm. We decided to use a worm gear system that will allow the user to adjust the tension of the elastic band with minimal effort, much like a guitar tuner. Given the nature of our design and the minimal force on it by the elastic band, we are not concerned with the gear system yielding. Our goal for this analysis was to determine the dimensions of each gear (pitch diameter, number of teeth, etc.) required so that the tension of the elastic band could be adjusted with a force of 1.5 pounds or less. We wanted to ensure this requirement is met such that the device remains accessible and users do not have to apply an unreasonable amount of force to tighten or loosen the device. We not only want to prioritize inclusivity by changing the tensile force in the elastic but also want to keep ease of use at the forefront of the design process. The mechanism is shown below in Figure 11.
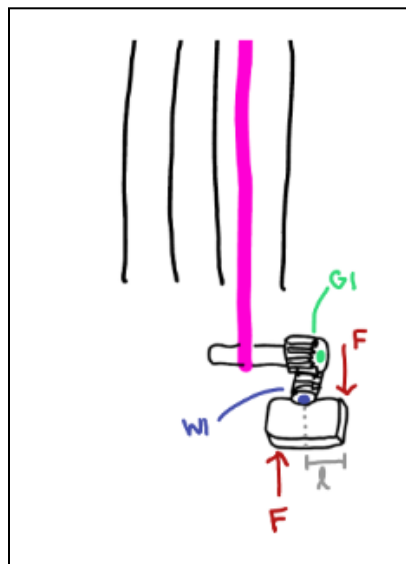

Figure 11
Diagram of Worm Gear Mechanism to Tighten Elastic

22

Using the following equation that relates input and output torques, we found the torque that the gear would experience from a user applying force on wingnuts of various lengths:

$$T_B = \eta \left(\frac{Z_B}{Z_A}\right)(T_A)$$

where Z_A and Z_B represent the number of thread starts on the worm and wheel respectively. T_A refers to the torque of the worm portion of the system and T_B refers to the torque of the gear as shown in the following figure:
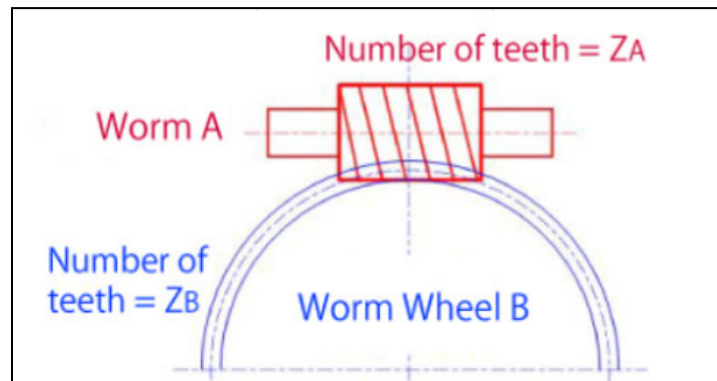

Figure 12

Visual Representation of Equation 3 (Source: Kohara Gear Industry, 2024)

From this, a pitch was decided on for both the worm and the gear such that they are compatible. This and the number of teeth on the gear were left as variables in a spreadsheet like many of the other values. Keeping parameters as variables allowed us to quickly analyze the efficacy of many different sizes and dimensions of components. However, to simplify our calculations, we entered preferred numbers for Z_A and Z_B as 1 and 18 respectively, as these are

commonly used values for guitar tuners (which our design is heavily inspired by). We also used

common sizes of tuning pegs as our basis for $R_{winding}$ to determine the torque necessary. The

data for different sizes of l and $R_{winding}$ has been tabulated below.

Table VI
Output Torque vs Required Torque for Various Worm Gear Setups

l (inches)	$R_{winding}$(inches)	Output Torque (in-lbs)	Required Torque (in-lbs)
0.1	0.125	1.671	3.125
0.2	0.125	3.342	3.125
0.3	0.125	5.013	3.125
0.4	0.125	6.684	3.125
0.5	0.125	8.356	3.125
0.1	0.172	1.671	4.297
0.2	0.172	3.342	4.297
0.3	0.172	5.013	4.297
0.4	0.172	6.684	4.297
0.5	0.172	8.356	4.297
0.1	0.203	1.671	5.078
0.2	0.203	3.342	5.078
0.3	0.203	5.013	5.078
0.4	0.203	6.684	5.078
0.5	0.203	8.356	5.078

This table allows us to compare many options and can be tweaked by altering the unshown values that are incorporated, like the applied force and gear ratio. Because we would like our design to be compact, we will likely utilize a smaller radius for the winding pin to try to keep a smaller twist handle length.

Given what we found through calculations and research, we are planning on designing or purchasing a worm gear mechanism with the following minimum specifications: one tooth (or thread) on the worm with 18 teeth on the wheel, with an output radius of 0.125 in and an input handle with a radius of at least 0.2 in. Doing these calculations helped us ensure that whatever mechanism we design is easy for a user to tighten with a small force applied using just the fingers.

Figure 13

Skeletal model of the hand and forearm given to us by Dr. Freilich. An initial prototype used as a reference guide when determining bone orientation, as well as the overall size and scale of additional components of our design (base and hand blocks).

In conclusion, we feel we have a thorough plan moving forward. Our numerous meetings with Dr. Forman and Dr. Freilich have highlighted what elements of a closed reduction are most important to replicate. Throughout the semester, through technical analysis and additional meetings, we've reached a design that we feel is viable and will be an optimal starting point. The entirety of the group is committed to starting as early as possible next semester on prototyping, which we anticipate will quickly highlight some unforeseen flaws in our design. However, given the adjustable nature of our current design, we believe that each iteration will be more a matter of small changes, rather than a complete redesign. In the future, we plan on continuing to actively meet with Dr. Forman, and we predict that it will be especially crucial to set up several meetings with Dr. Freilich. His expertise and experience in manual reduction is what will allow us to get feedback on the feel of our device and tweak it so that the motions of reduction are accurate. Additionally, as our design approaches its final iteration later in the semester, we hope to potentially partner with UVA medical students to get their input on how well our design has replicated a closed reduction.

Final Specifications

In our initial specifications list, we listed 21 specifications of varying levels of importance that we wanted to incorporate into our device. While our initial specifications guided us throughout our design process, several specifications were changed or dropped as we developed our device. These changes along with the achieved specifications are detailed in Table VII.

Table VII
Final Specifications for Wrist Fracture Reduction Simulator

Initial Specification	Description	Metric	End Result
Skin Feel	The "skin" of the simulator must feel realistic enough to allow for accurate training (grippy enough, but pliable)	Subjective tests by engineers and physicians	Achieved. Skin deemed realistic by Dr. Freilich.
Skin Elasticity	The "skin" must stretch and bend similar to human skin	Percent elongation and modulus of elasticity testing	Achieved. Silicone skin is extremely elastic, beyond adequate for our needs.
Skin Durability	The "skin" should be durable and last through many uses of the simulator	Count number of cycles at greater than expected stress	Achieved. Only possible issue is the zip ties not being oriented correctly and cutting through silicone.
Cost of Production	Summed cost of producing/ordering must be less than or equal to $150.	Cost in US Dollars	Achieved. Final Cost of $50.08.
Force Variation	Force required to "set" wrist must be variable (i.e. tensions in soft tissue)	Run tests with different desired forces and ensure that the force required to move the simulator varies	Achieved. Variable force was achieved with elastic attached to guitar tuners.
Accessibility of Materials	All materials must be available to a common person	List of retailers that materials can be purchased from by average person	Achieved. All materials are able to be acquired from sources like Amazon, Lowes, etc.

Ease of Construction	Simulator must be able to be constructed with a set of instructions once all materials are gathered	Give instructions and materials to random participants and measure the success rate	Achieved. Instruction Manual provided.
Accurate Bone Orientation	Initial position of "bones" must be accurate to a typical distal radius fracture	Comparing physical simulator to x-ray image of distal radius fracture and physician feel	Achieved. Accuracy of bone orientation confirmed by Dr. Freilich.
Realistic Fracture Reduction Force	Bones should only be able to move from a "stable" to "unstable" after minimum precise force is applied	Force required to "set" fracture	Achieved. Accuracy of reduction feel confirmed by Dr. Freilich.
Replicable	Design ensures every simulator made will be nearly identical	Meeting specifications on multiple models	Achieved. Process to replicate the device is detailed in the instruction manual.
Resettable Configuration	Must be able to reset the simulator after performing the reduction	Perform cycle testing to make sure the simulator can be reset to the original position without breaking or losing stiffness	Achieved. Device can be returned to fractured state easily.
Ability to Calibrate	Can measure and indicate the amount of force necessary for different variations of fracture reduction and variable forces required	Use force gauge to record required force for each calibration and compare it to simulators reading	Achieved. Tensions in the elastic bands are detailed in the instruction manual.
Easily Adaptable for	Simulator can be	Number of different	Not achieved. In case

Different Fracture Types	modified with minimal effort to simulate different types of fractures	fractures it could be potentially compatible with and how many steps swapping the model takes	of new fracture patterns being developed, modifying the fracture pattern would require taking the entire device apart and reassembling it.
Physical Verification	Ability to physically verify that the fracture reduction was performed correctly	Indication of successful reduction exists and is corroborated by trained physician	Achieved. Viewing hole allows the user to verify that reduction was successful.
Ability to Splint or Cast	The simulator must be able to have a splint or cast applied to it by students	Setting and removing a cast and ensuring there is no damage to simulator	Achieved. Device's bridge allows for splinting.
Weight	The simulator must weigh a similar amount to the limb of a similar size	Measure weight with scale	Dropped. Given that the device is clamped to a table, the weight of the device is irrelevant.
Scalable Simulator	The simulator can be easily scaled to create smaller or larger models to accurately simulate different sized people	Measure the components of each sized simulator and compare it to anatomical data of the corresponding demographic of people	Partially Achieved. Device design can be altered to scale bones with minimal CADing work.
Two Equilibriums	Has to reach a static equilibrium in both 'broken' and 'set' positions	Test both broken and set positions to ensure the device is stable and will not deviate from equilibrium with minimal forces	Achieved. Orientation of elastic bands achieves a dual equilibrium.

Accurate Reduction Motion	The motion required to use the simulator is the same as seen in real patients	Physician feel	Achieved. Accuracy of reduction feel confirmed by Dr. Freilich.
Compatible with Current Technology	Should work with splints, finger traps, etc.	Get physician to try some of their current methods out with the simulator and measure the success rate	Partially Achieved. Device is compatible with splints but not finger traps. Dr. Freilich was satisfied with our device having a fingerless hand.
Interchangeable Components	Ease of swapping specific parts such as bones or mechanical components to ensure easy repair	"Break" the simulator and measure the ease and amount of parts to fix it	Partially Achieved. Parts are easy to replicate/come. Depending on which part is broken, replacing a part might require taking apart and reassembling the entire device.

Finite Element Analysis (FEA)

Because the shape of the bones is quite complex, we decided to perform finite element analysis (FEA) on them to determine if there are any weak spots. When FEA was performed on our initial design, it was determined that the likely point of breakage was on the ulna. This makes sense because the ulna is the thinnest part of the design and is subject to the most stress during the reduction process. For this reason, when performing the FEA for the final design, we elected to focus on the ulna only.

The ulna was constrained at the base, and vertical and horizontal 10 lb loads were applied at the top. 10 lbs was chosen since the actual force will be roughly 20 lbs, but will be applied to two bones instead of one. When performing FEA analysis on the initial design, ABS plastic was selected, but because the final design was made of PLA, the material for the FEA in this scenario was PLA (Polylactic Acid). The material properties of PLA are shown below.

Figure 14
PLA Material Properties
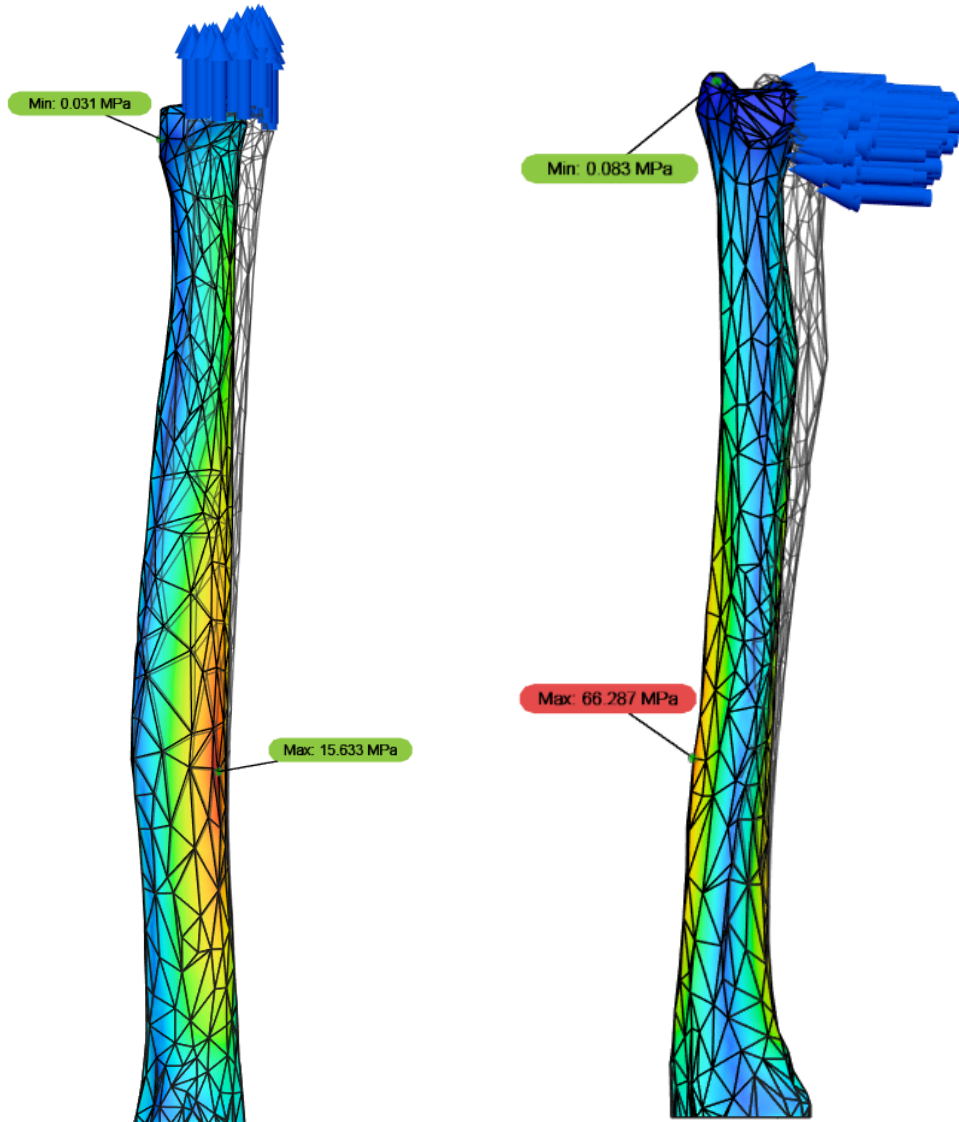
Figures 15 and 16
10 lb Tensile Force and 5 lb Bending Force
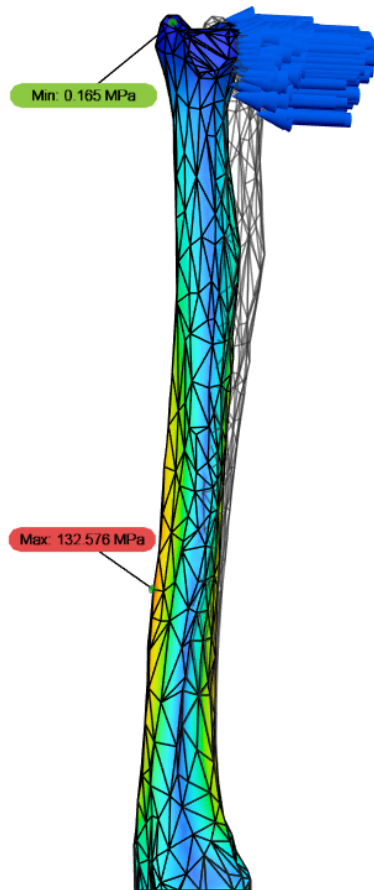
Figure 17
10 lb Bending Force

These results demonstrate that the weakest point in the design is roughly two thirds down the ulna, which makes sense when considering the thinness and distance from the applied force. Because these stresses are so high, it is important for the device users to ensure that they are being mindful of how much force they are putting on the device. The most risky part of the reduction on our device occurs when pushing or pulling horizontally during the initial phase of the reduction. If issues were to occur in the future, an easy fix would be to change the infill pattern or thickness of the bones in the high stress areas.

Bending Calculations

While our model was being tested by Dr. Freilich, there was a large amount of force being applied to the bones in a tangential direction as he was using his other hand to hold the bones in place while reducing the fracture. To ensure that there would be no failure due to the bending moments created by this tangential force, we performed calculations to determine if our model could withstand that force.

The perform these calculations, we treated both the radius and ulna as cantilevered beams under the following loading conditions:
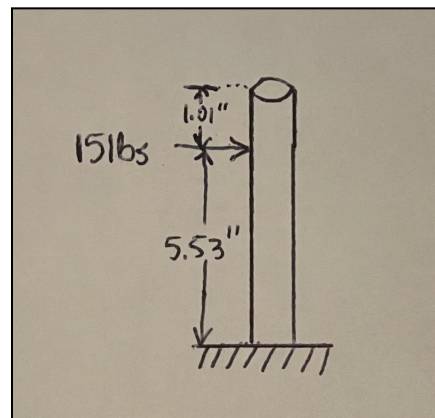
Figure 18
Loading Conditions for Bending Calculations

A 15 pound load was selected for this calculation because even though the axial force to reduce a distal radius fracture can be up to 25 pounds, this tangential force is likely to be half of that force or less. Next, we calculated the maximum bending moment present in each bone using the moment diagram in Figure 19. This maximum moment was found to be 82.95 in-lb at the base of the bone.
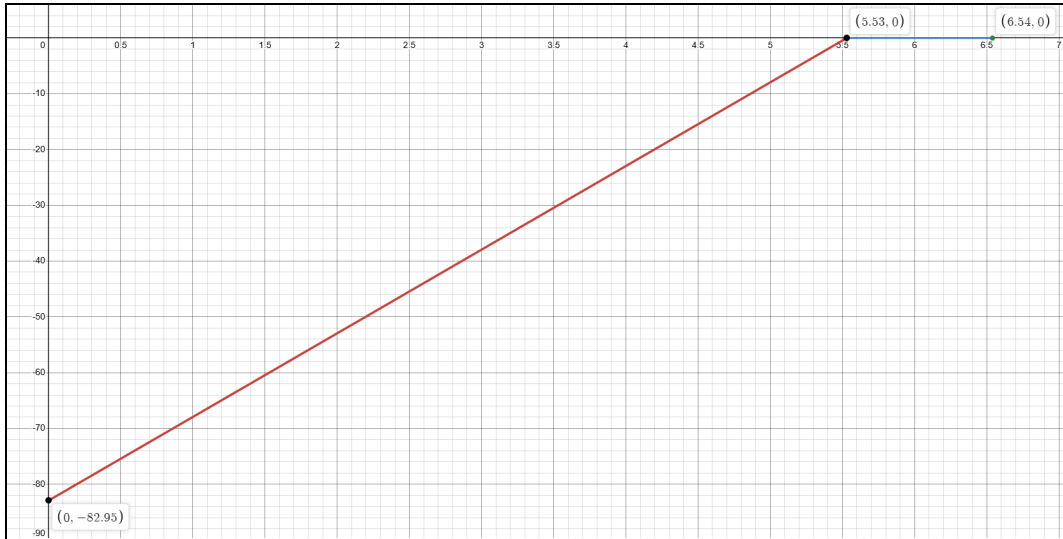
Figure 19

Moment Diagram for Internal Bending Moment of Radius and Ulna

Using the diameters of the radius and ulna at their bases, 0.605 inches and 0.693 inches respectively, we could the use the bending stress formula, $\sigma = \frac{Mc}{I}$, to calculate the stress due to bending. To find the maximum stress, c was set equal to the radius of each bone, and I was found using the formula $I = \frac{\pi D^4}{64}$. Using these values, the maximum stress in the radius was found to be 3.815 ksi and the maximum stress in the ulna was found to be 2.539 ksi. The tensile strength of PLA is known to range from 39.9-52.5 MPa, or 5.79-6.61 ksi, which is much higher than our calculated stresses, showing that our simulator will not experience failure due to bending.

Tensile/Failure Testing

One key aspect of our model was the feel of the reduction and therefore the correct tensioning of our elastic bands. After we developed our model and got Dr. Freilich to test and approve the design and feel, we wanted to get a better understanding of the force distribution throughout the various elastics in the model. To do this we used the setup shown in Figure 20

35

and a force sensor attached to the top knot of each of our 4 elastics. The measurements that for the individual bands are shown in the table below:

Table VIII
Force Measurements of Varying Elastics

Location of Elastic	Approximate Tension (lbs)
Medial - Palm	3.05
Medial - Dorsal	5.95
Lateral - Dorsal	4.6
Lateral - Palm	2.7
Total (all four)	**16.3**

Figure 20
Setup for tensile testing of the 4 different elastics

The resulting total force of around 16 lbs seems fairly reasonable as from previous research and conversations with Dr. Freilich we found that reduction forces could be in the range of 15-25lbs. Our model is on the lower end of this, and that could be explained by the fact that the silicone skin also adds a bit of force necessary to reduce the fracture. Additionally, someone with a smaller stature, like a female or younger adult might fall on the lower side of this spectrum. After ensuring that our numbers made sense we wanted to find a way to correlate the number of turns on the tuner to the tension in the elastic. To investigate this we decided to untie one elastic from the fracture and gather a range of measurements on the number of turns and the correlating increase in tension. The setup for this process is shown in Figure 21 and will allow users to understand and calculate the number of turns they will need to do to get a desired force. Note that this number can be controlled by changing the initial length which was 30 cm for the test we did.
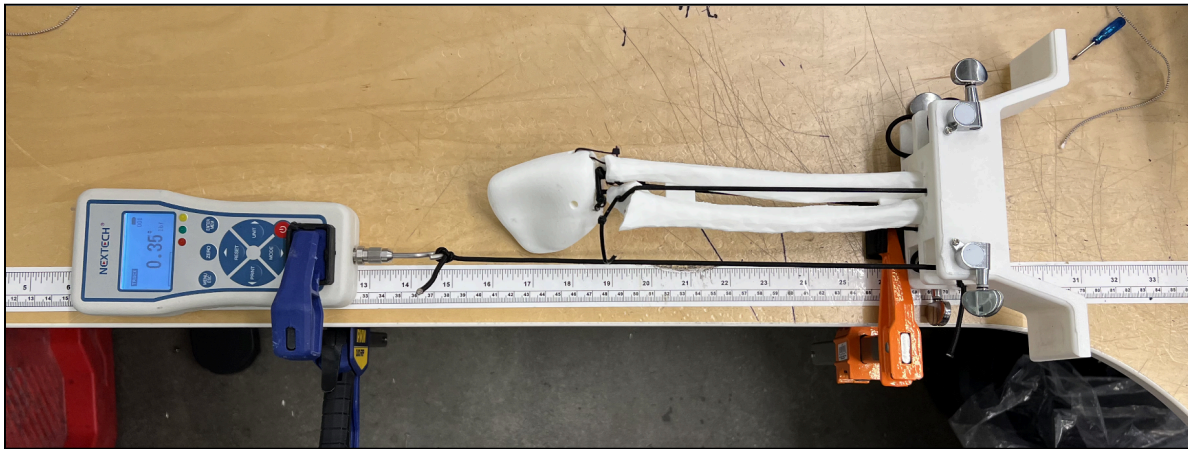

Figure 21
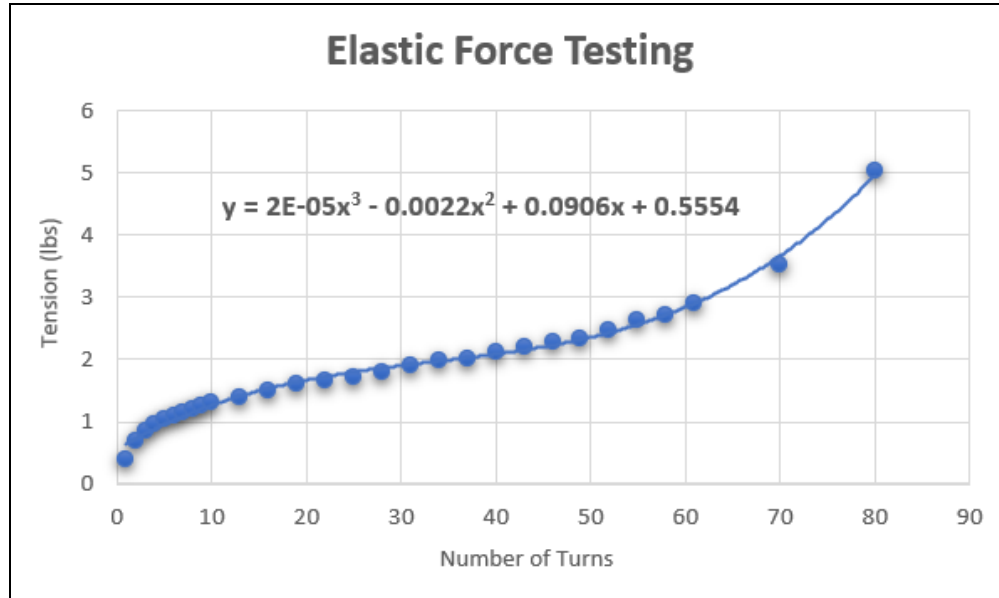Setup for correlation of tuner rotations and resulting elastic force

Figure 22
Plot of number of tuner turns vs. tension

The above figure shows a pretty clear relationship between number of turns and tension. The data points collected were able to be represented very well with a 3rd degree cubic polynomial. Moreover, from about 15 turns to 60 turns, the function seems to be relatively linear, which will make it easy for users to pick a suitable length, tighten their model to a chosen tension, or reproduce characteristics that are similar to our model. The model did end up 'failing' at about 80 turns, but nothing actually broke. The small screw attaching the tuner to the base managed to unscrew itself because of how much elastic was on the tuner axle (80 turns). The model was easily fixed as there was no real damage. This taught us that it is better to increase the tension of the elastic initially when the knots are tied then to wind the elastic around the axle an excessive number of times. Other than this, our model showed great resilience.

Qualitative Analysis

While we did do some numerical and quantitative analysis, one of the main portions of our project was qualitative and involved feedback from an orthopedic surgeon. In the section below we will dive into the iterative prototyping process of each of the different parts of our model. This will explain why we made the decisions that we did and what kind of qualitative feedback we based our changes upon.

Tuners

One potential cause of failure of our design is in the guitar tuners. If too much tension is present in the elastic cables, there could be a failure in either of the gears internal to the tuners or in the shaft of the tuner. However, guitar strings are typically under a tension of up to 35 pounds, while our elastic cables will only need to be under 6-10 pounds each to accurately simulate a distal radius fracture reduction. Due to this large difference in tension, and the factor of safety already built into the guitar tuners, the risk of failure due to excess tension on the tuners is negligible.

In addition to failure, our objectives included making it easy to change the tension in the simulator. With our tuners providing a gear ratio of 15:1, and the elastic only holding 6-10 pounds in tension, the maximum force that a user would need to apply to change the force would be less than a pound, which should be very easy for anyone using the device. While our original plan was to 3D print worm gears, the strength of the plastic was a concern along with difficulty of assembly and we wanted to make sure it was simple for users to reproduce and that the model was durable. Guitar tuners proved to be an effective solution to both of these issues and we knew that they would be able to withstand the necessary forces.
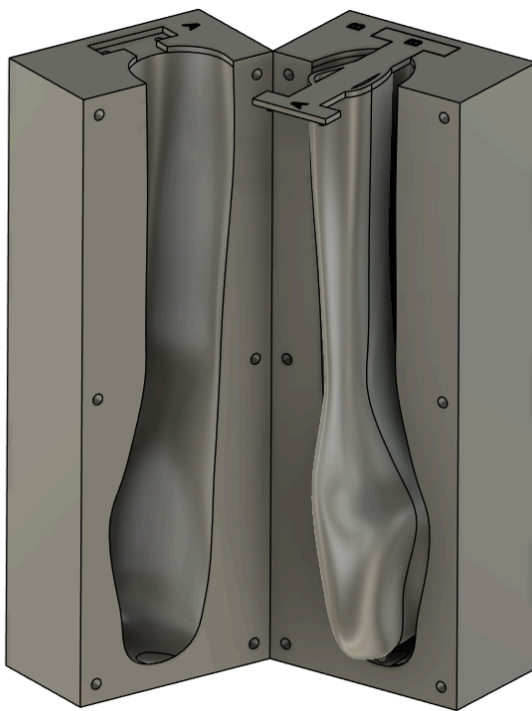
Silicone

In order to make the model feel like it was covered in skin and flesh, we had to make a silicone "skin" to cover it with. The original silicone purchased was an inexpensive option, but when cured, it was extremely stiff and not stretchy. Another issue with the first silicone was that it was extremely smooth and shiny, and the plastic feeling was not conducive to a skin-like exterior. If this silicone were to have been used in the final design, it would have been difficult to manipulate the fracture and perform the reduction, and it would not have felt like skin. Because of this, a more expensive, softer silicone was chosen.

Silicone comes in two variations - platinum-cured and tin-cured. Platinum-cured silicone is longer-lasting, higher quality, and more durable than tin-cured silicone, which is why we selected platinum-cured silicone for use in our model. The main downside of platinum-cured silicone is that it is susceptible to cure inhibition, which is when silicone fails to fully cure, leaving it sticky, tacky, or even liquid. When using our original 3-D printed molds, there was a reaction with the PLA that led to cure inhibition of the silicone. For this reason, we obtained a mold releasing agent that was used to seal the PLA molds before pouring the silicone.

One of the other challenges when designing the silicone "skin" was creating the mold. Because the hand portion of the model is wider than the bones, it was difficult to create a mold that allowed for a tight fit around the entire model. An inner section of the mold, in the shape of the hand and bones, was placed inside an outer two-part mold and attached at both ends before the silicone was poured into the mold. At first, the inner portion of the mold was only attached to the outer mold at the "elbow", but the slanted angle of it led to the silicone pooling at one side and making the silicone too thin on one side of the model.

The final challenge that the silicone posed was finishing it so that it was not tacky or sticky to the touch. We found that when you take the silicone out of the mold, it has a smooth finish but is sticky enough that dirt and hair adhere to it and it sticks slightly to one's hands. After some research into how people care for other silicone items such as dolls and phone cases, it was found that after cleaning the silicone with isopropyl alcohol and letting it dry, adding a thin coating of cornstarch, thoroughly brushing off any excess, gives the silicone a soft, skin-like finish. This cleaning and finishing process can be repeated as needed, but will likely last without the need for retouching for several weeks. The final mold and model with silicone are shown in the figure below:

Figures 23 and 24
CAD Model of Silicone Mold, Finished Silicone on Model

Equilibrium State

To accurately replicate the mechanics of a distal radius fracture, the model was designed with a key constraint that it must exhibit two distinct states of equilibrium. These states are defined as the set state and broken state. In this context, equilibrium refers to a condition in which the forces acting on the fractured segment do not cause any movement in either state. Therefore, the fracture occupies a distinct position in the broken state that must be physically manipulated to transition into the set state where it remains. In the broken state, the elastic bands apply tension to both the dorsal and palmar sides of the hand, and a significant force is required to overcome the broken equilibrium and reposition the fracture into its correct set alignment. The appropriate level of tension to accurately simulate the feel of reduction was determined through an iterative process, guided by feedback from orthopedist Dr. Freilich. Adjustments to the line of force, tension, and fracture pattern were made throughout the process, with periodic testing and input from Dr. Freilich to enhance the model's realism. One challenge in designing the equilibrium states was introducing a degree of instability into the set state. In clinical practice, it is common for the set position to experience a level of instability and play, which is typically counteracted through the application of a splint. Designing a fracture geometry that possessed two states of equilibrium while incorporating controlled instability in the set position proved challenging and is discussed further in the following section.

Fracture Geometry

One of the most difficult and important design components of this project was fine-tuning the fracture pattern. As mentioned previously, it was very important that the device have 2 states of equilibrium and facilitate movements that felt like a real reduction. One of the difficulties here

was designing the fracture line such that it created the necessary movement, yet still remained in a random pattern as a natural fracture would. The process of designing the fracture pattern in Tinkercad will be detailed below.

The location and orientation of the fracture were decided by looking at several different x-ray images of Colles' fractures and deciding on the approximate design. In Tinkercad, the scanned model of the forearm bones was imported and the orientation of the radius and ulna with respect to each other was kept in its natural state. The fractures are arranged such that the location of the fracture is close to the working plane, making it easier to edit (Figure 25). The fracture design itself is made by utilizing the 'terrain' feature that is essentially a random array of jagged divisions whose smoothness and variability can be changed (Figure 26). Changing the smoothness of the fracture line allows the difficulty of the reduction to be controlled. A more jagged fracture pattern would be more stable, and a smoother pattern is a lot more unstable and might necessitate medical students to practice splinting the bone. To create the fracture in Tinkercad, the terrain is set to 'hole', and the bones and the terrain are grouped together.
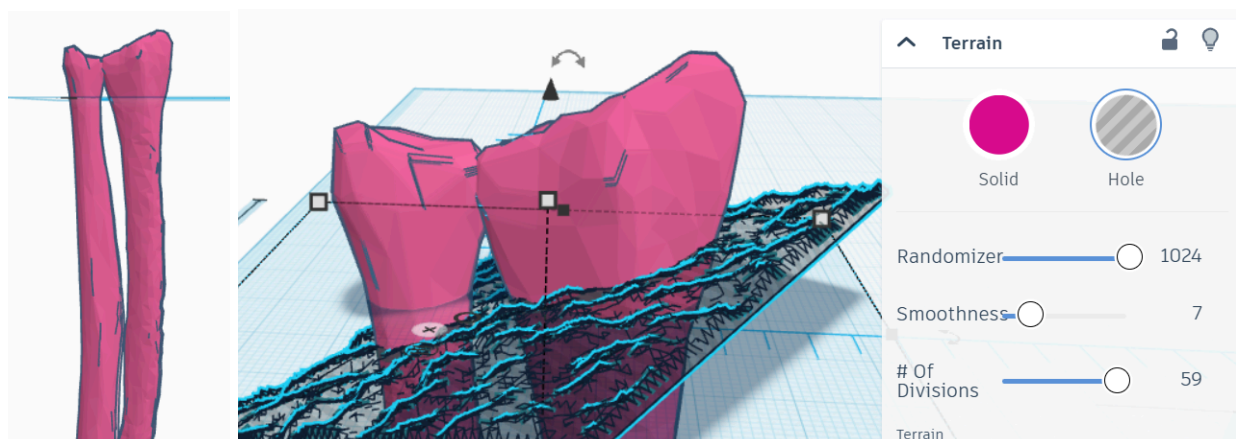

Figures 25 and 26
Far Out and Zoomed in Demonstration of the Terrain Feature

After making the initial cut the model should look like below (Figure 27). Now the goal is to remove all of the other material that is not the fractured piece of the radius. This is done using various shapes and the 'hole' setting, and then grouping everything together (Figure 28). This will give us the lone, 'positive' fracture piece that we can now use to cut into the bones and create a 'negative' indentation on the bones that the fracture piece will fit perfectly into. After this, the grid snap is turned off such that the measurements are exact, the ruler feature is turned on, and the fracture piece is moved to the coordinates (0,0) (Figure 29). Now, duplicate the fracture piece and move it 100 mm up to get it out of the way. Now ungroup the bottom model and delete all of the shapes used other than the bones themselves (Figure 30).
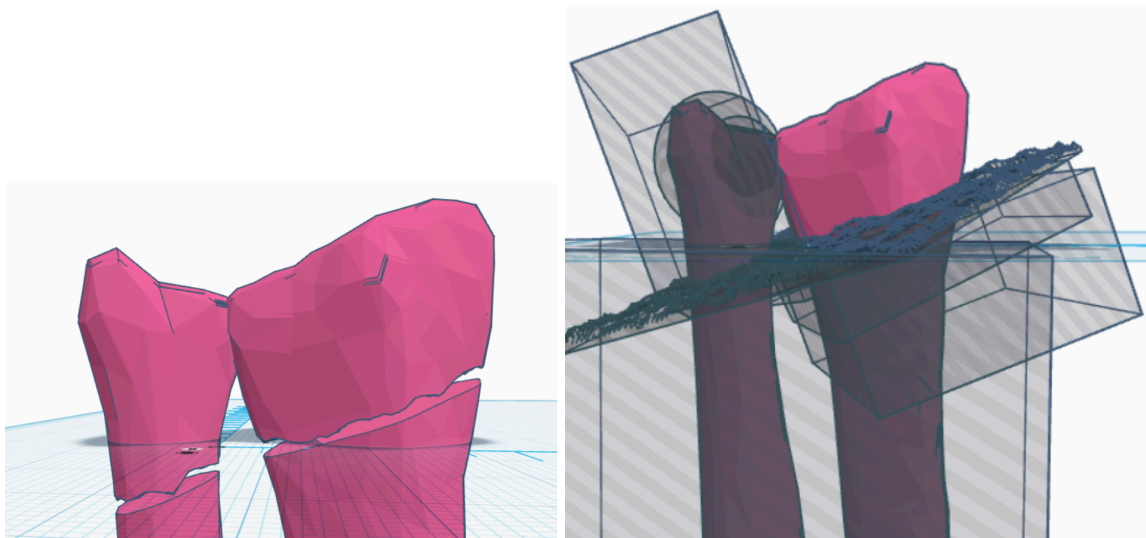
Figures 27 and 28
After the Initial "Cut", Grouping All Extraneous Parts Together
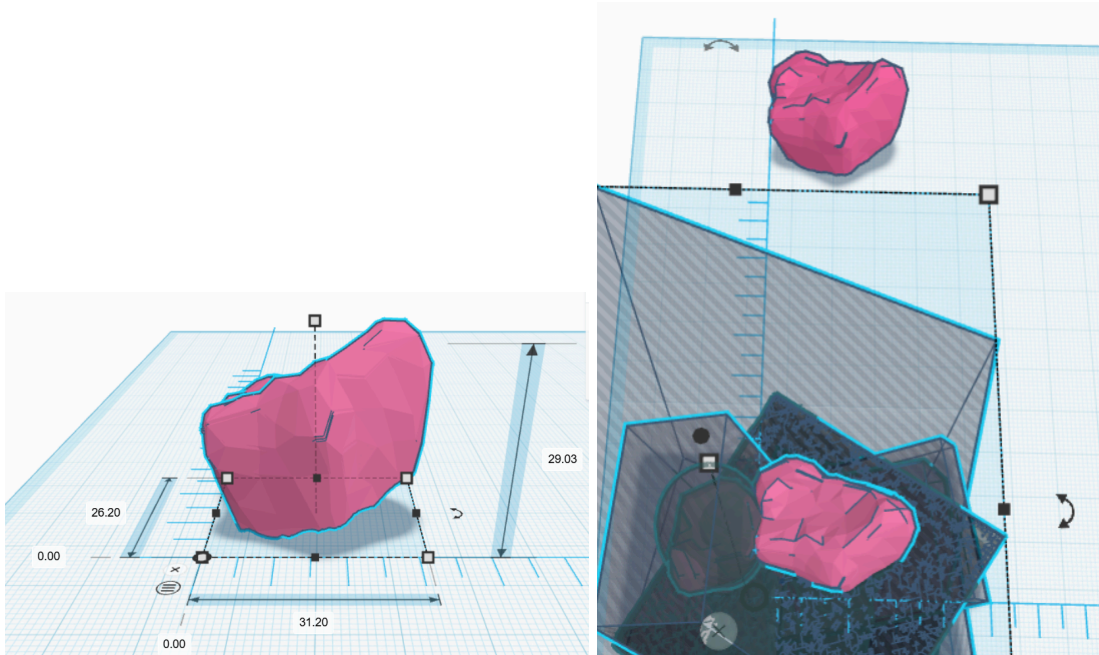
Figures 29 and 30
Moving the Fracture Piece to the Origin, Deleting All Unnecessary Parts

After all of the extraneous shapes have been deleted, change the color of the untouched fragment and move it back down 100mm such that it perfectly overlaps the bones (this is why we turned off grid lock) (Figure 31). Duplicate the lone fracture piece one more time and move it out of the way, then set the remaining fracture piece (shown in green) to be a 'hole' and group the two pieces of the model together. Depending on the model, you may need to size up the dimensions of the cut very slightly to ensure all of the original bone material is removed. After doing this the fracture should like something like (Figure 32)
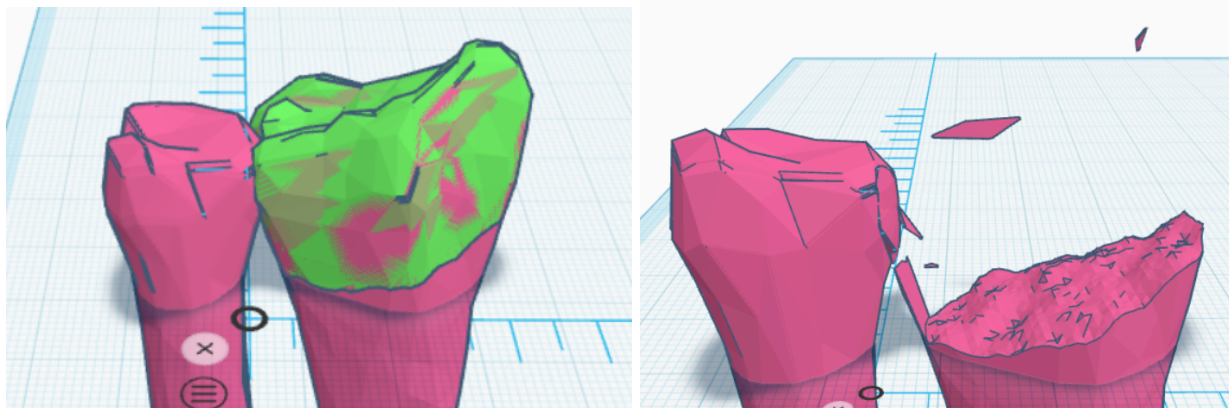
Figure 31 and 32
Overlaying the two fracture pieces, grouping the pieces together

To remove the jagged edges and unwanted fragments, use shapes set to 'hole' like we've done in the past until the model looks how you want it. After this, both the fragment piece and the broken bone pieces are complete and can be exported into your main CAD software.

Hand design

When a reduction is performed, doctors grip onto the palm of the patient's hand to pull the bones back into place. When we were creating our design, we decided that the most simple but still accurate way to create a "hand" for the device would be to shape the palm part and omit the fingers. This is because the fingers would either end up too stiff or too flexible depending on whether they were solely silicone or had a plastic core. Originally, a simple trapezoidal "hand" was created, but this was soon changed in favor of a more accurate design based off of a group member's hand. First, her hand was scanned using an app that converts 3-D scans into STL files. After the mesh was applied to smooth it, we decided to "cut off" the fingers and smooth out the remaining palm part. This scanning and smoothing process can be seen in the images below.
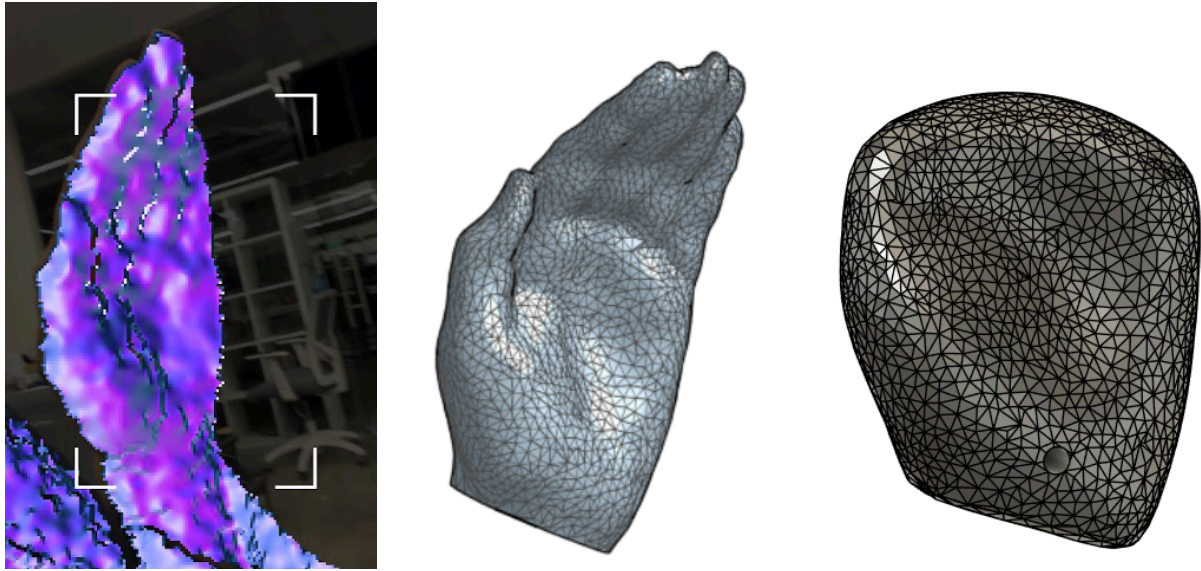
Figures 33, 34, and 35
3D scanning process, scanned STL of hand, final hand design cleaned up

The final hand design has the contours of an actual palm, including the ridge where the

thumb is. These contours allow doctors to grip onto the model as they would an actual hand.

Additionally, holes were added to the final "hand" so that it could be properly

Base Design

The base of the model was designed to incorporate multiple functional features, each

contributing an element necessary for realistically simulating reduction. The primary structural

components include a rectangular base plate, two angled legs extruding from the base plate, and

flanges at bottom of each leg that lie parallel to the base plate. The base plate features

indentations contoured to match the shape of the two bones, allowing them to sit securely and be

fastened with screws inserted beneath the base. Additionally, holes are distributed around the

perimeter of the base plate to allow attachment of the elastic bands. There are 14 holes for the

four elastic bands, providing flexibility in adjusting the path of tension. The base plate also features four channels, each containing a hole designed to press-fit an axle securely into a channel. Each axle is connected to a guitar tuner, which enables individual rotation of an axle. Each elastic band is secured to an axle to allow them to coil around the axle as the tuner is rotated, thus providing control over the tension applied to each individual band.

The flat sections on either side of the base serve as the contact points between the model and mounting surface. These flanges provide sufficient surface area to attach standard c-clamps, allowing the model to be securely fastened to work space. This feature provides the stability required for practitioners to apply controlled force during the reduction. The angled legs elevate the base plate, creating a gap between the model and underlying surface. This design creates space for practitioners to pass plaster under the model and up along both sides of the arm, simulating the application of a splint. The bottom of the base plate acts as an anchor, similar to an elbow in real life, enabling splinting practice after the reduction to emulate the subsequent stabilization of the wrist. Straight edged surfaces – such as junctions between the legs and base plate or flanges, channel walls, and edges of the base plate – were filleted to minimize stress concentrations. Collectively, these design characteristics of the base provide distinct functionality necessary to achieve the overarching goal of accurately replicating the tactile experience of reduction.
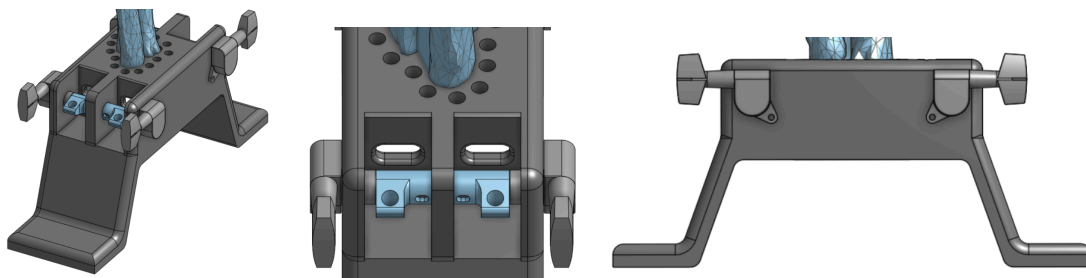

Figures 36, 37, and 38
Base Isometric View, Base Guitar Tuner and Channel View, Base Side View
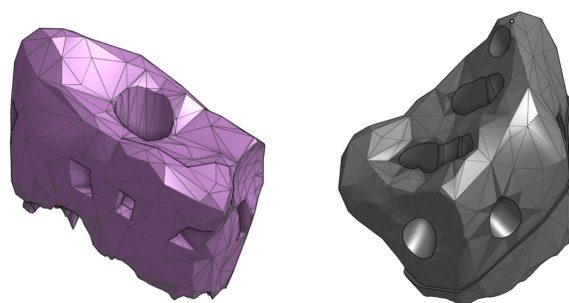
Testing

As stated prior, we were relying heavily on Dr. Freilich and Professor Forman to help test our device to ensure it achieved the feel of a real radius fracture. With their guidance, we continuously altered our design throughout the semester, keeping in mind our specifications as we progressed.

The most notable specification that was met via testing our prototype was achieving an accurate reduction feel and process. This can be seen in several areas: the points at which the elastic were attached, the differing tensions within the elastic bands, and the fracture pattern. The change in the elastic band placement can be displayed through the evolution of the base and the holes on the fracture; both initial versions of the base and fracture had an excessive number of holes to allow different configurations in order to determine the one that would provide the most realistic reduction feel. Once these had been determined, the number of holes on the base and the fracture were limited to only those that were required. The differing tensions in the elastic bands were achieved using separate guitar tuners for each elastic band. We determined the specific tensions within each of these bands through presenting the prototype to Dr. Freilich and letting him adjust the model until he was satisfied with the reduction feel. The fracture pattern was altered throughout testing due to our initial fracture pattern being too stable in the reduced state. We flattened out the fracture to make it less stable in the reduced position, resulting in the model needing to be splinted to keep the fracture in its proper position. The changes in the base design can be seen in figures 39 and 40, the changes in the fracture pattern can be seen in figures 41 and 42, and the changes in bone design can be seen in figures 43 and 44.
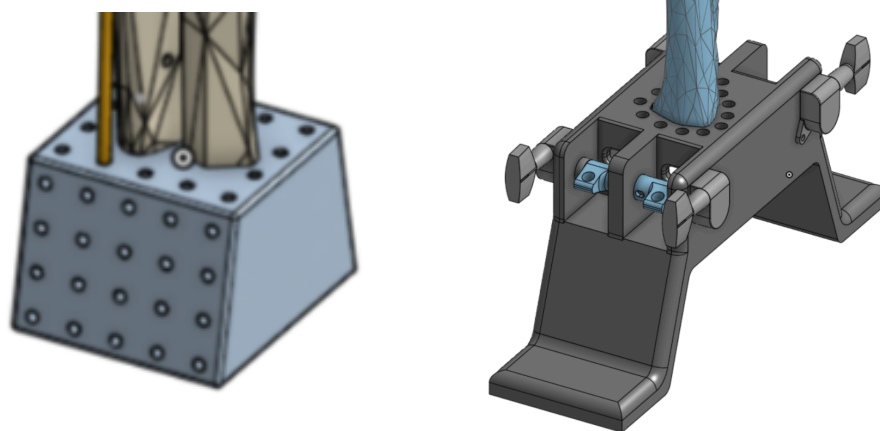
Figures 39 and 40
Initial Base Design, Final Base Design

Figures 41 and 42
Initial Fracture Design, Final Fracture Design
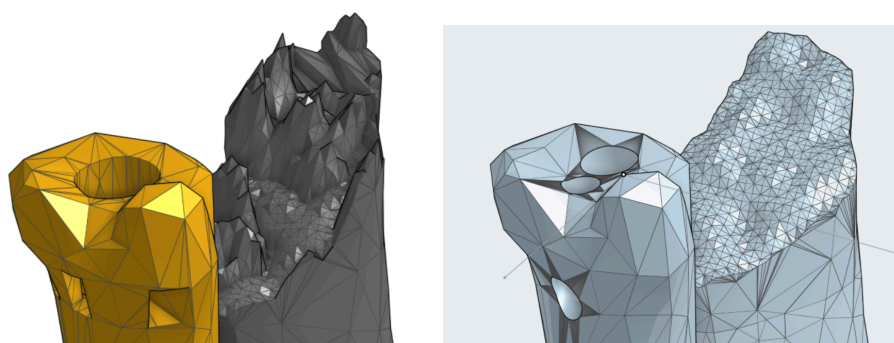
Figures 43 and 44
Initial Bone Design, Final Bone Design

Another specification that required repeated testing to achieve was the skin feel. This included testing multiple types of silicone to determine which was the most elastic, durable, and accurate feeling. Once we had determined the optimal silicone to use, multiple tests were required to optimize the mold pattern to create a silicone layer that was thick enough to withstand repeated use while remaining accurate in feeling. The changes in the mold design can be seen in figures 45 and 46.

Figures 45 and 46
Initial Silicone Mold Design, Final Silicone Mold Design

Conclusion/Future Work

Overall, our project was a success. Our training device only costs $50.08 to replicate and only requires easily attainable materials and tools to construct. The accuracy of our device's reduction process and feel was approved by an orthopedic surgeon. Essentially all of our initial specifications were achieved, with only one being deemed unnecessary, and the few that were not achieved falling within the realm of future work.

This project has shed light on a number of opportunities for future improvements and modifications. While the current iteration is satisfactory in terms of its design and feel, more time could be spent perfecting the tactile portion of the design, which is the most critical component for making this a device that could be useful to medical students. Meeting with other orthopaedic surgeons and getting their opinion on our design would allow for more fine tuning of the prototype, specifically the strength of the elastic bands and the stability of the fracture piece mentioned above.

Additionally, future work could be invested in similar devices that target other fracture types or dislocations. Closed reduction is used for a number of other injuries, including clavicle and ankle fractures, femur fractures in children, and is part of the process for fixing hip dislocations. Creating devices that accurately mirror these procedures could drastically improve physicians proficiency in setting fractures and could reduce the amount of teaching that has to be done on live patients.

APPENDIX

References

Corsino, C. B., Reeves, R. A., & Sieg, R. N. (2023). *Distal Radius Fractures*. StatPearls.

    https://www.ncbi.nlm.nih.gov/books/NBK536916/

Distal radius fracture reduction algorithm. University of Virginia School of Medicine. (n.d.).

    https://med.virginia.edu/orthopaedic-surgery/wp-content/uploads/sites/242/2015/11/Dista

    l-Radius-Fracture-Reduction.pdf

Dixon, W., Miller, N., Toal, G. G., Sebok-Syer, S. S., & Gisondi, M. A. (2020). Development of

    a 3D printed simulator for closed reduction of distal radius fractures. *Perspectives on*

    Medical Education, *10*(3), 192–195. https://doi.org/10.1007/s40037-020-00609-w

Graff, S., & Jupiter, J. (1994). Fracture of the distal radius: Classification of treatment and

    indications for external fixation. *Injury*, *25*.

    https://doi.org/10.1016/0020-1383(95)90125-6

GTSimulators. (2024). Transverse Colles' Distal Radius Fracture Model. GTSimulators.Com.

    https://www.gtsimulators.com/products/hm-fx-reduction-trainer-transverse-colles-distal-r

    adius-fracture-model

Handoll, H. H., & Madhok, R. (2003). Closed reduction methods for treating distal radial

    fractures in adults. *Cochrane Database of Systematic Reviews*, *2010(1).*
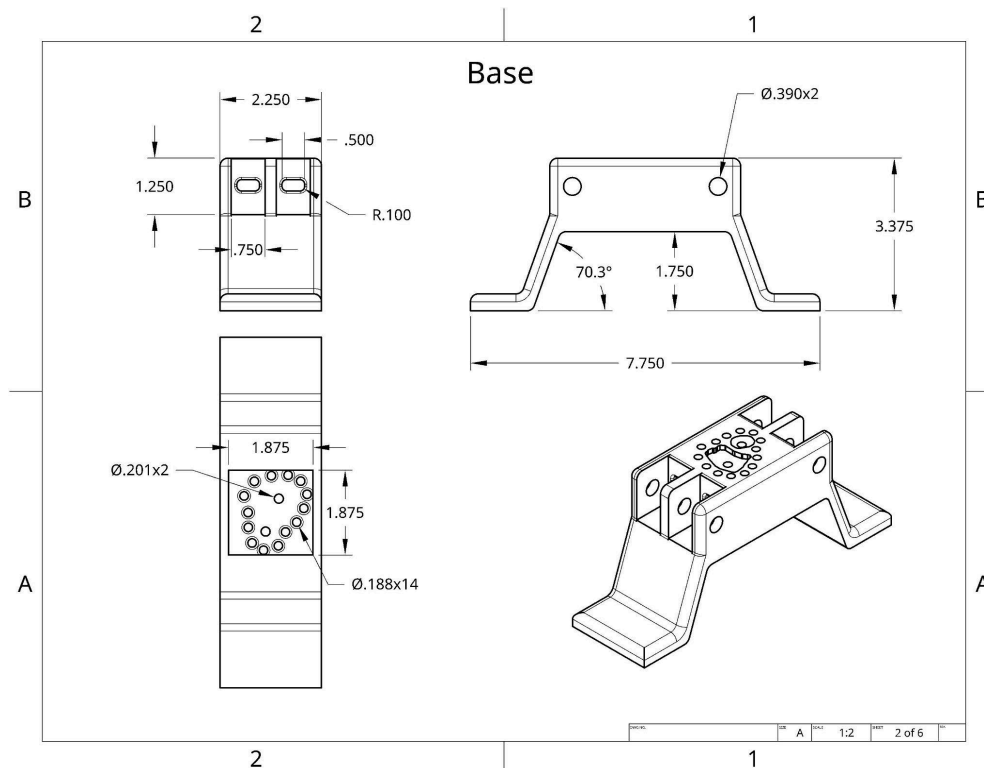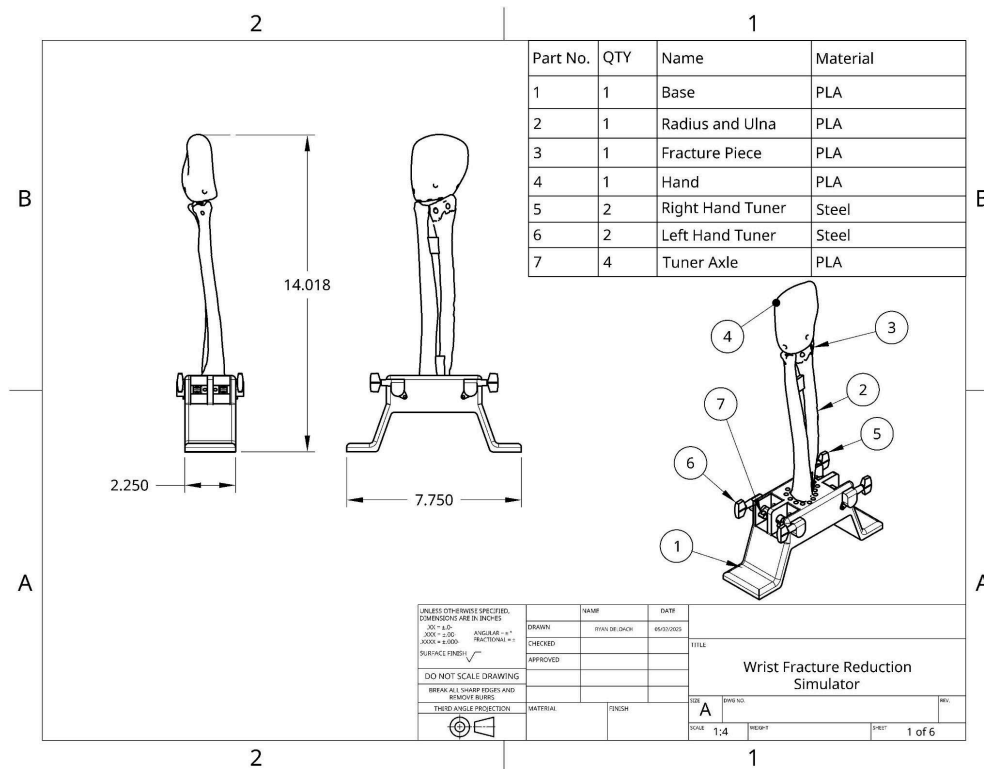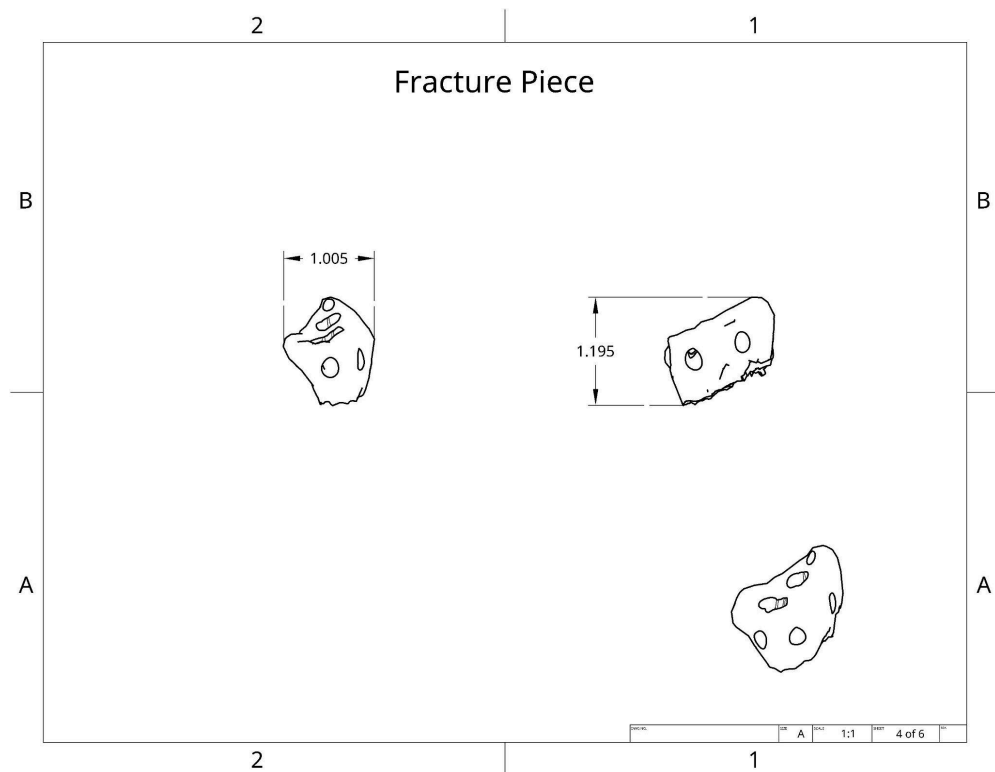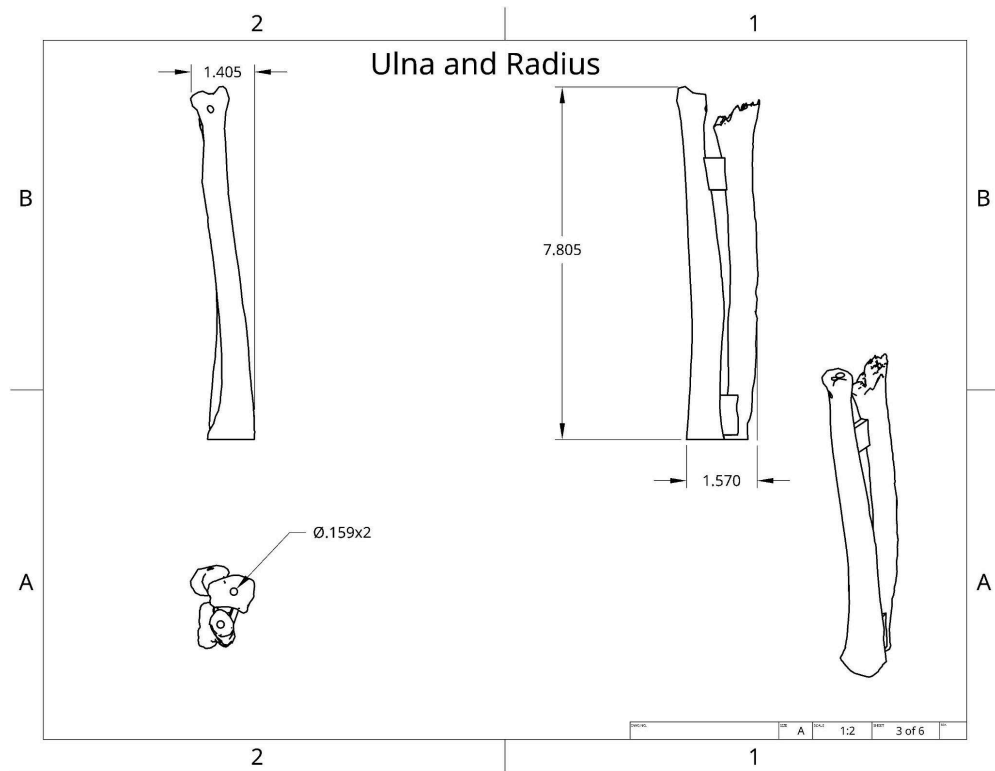
    https://doi.org/10.1002/14651858.cd003763

Jackson, T. J., Shah, A. S., Buczek, M. J., & Lawrence, J. T. (2020). Simulation training of

    orthopaedic residents for distal radius fracture reductions improves radiographic

    outcomes. *Journal of Pediatric Orthopaedics*, *40(1)*.

    https://doi.org/10.1097/bpo.0000000000001387

Kohara Gear Industry Co. (2024). Know about gear transmission torque. KHK Gears.

    https://khkgears.net/new/gear_knowledge/the-first-step-of-mechanism-design-using-gear

    s/know-about-gear-transmission-torque.html

Koh, S., Andersen, C. R., Buford, W. L., Patterson, R. M., & Viegas, S. F. (2006). Anatomy of

    the distal brachioradialis and its potential relationship to distal radius fracture. *The*

    Journal of Hand Surgery, *31(1)*, 2–8. https://doi.org/10.1016/j.jhsa.2005.08.012

Lateef, F. (2010). Simulation-Based Learning: Just like the real thing. *Journal of Emergencies,*

    Trauma, and Shock, *3*(4), 348–352. https://doi.org/10.4103/0974-2700.70743

Limbs & Things. (2024). Colles' Fracture Reduction Trainer. Limbs & Things.

    https://limbsandthings.com/us/products/70250-colles-fracture-reduction-trainer-light-skin

    -tone/

Nellans, K. W., Kowalski, E., & Chung, K. C. (2012). The epidemiology of distal radius

    fractures. *Hand Clinics*, *28(2)*, 113–125. https://doi.org/10.1016/j.hcl.2012.02.001

Nema, S. K., Austine, J., Ramasubramani, P., & Agrawal, R. (2023). Ultrasound-guided

    manipulation does not prevent malalignment over landmark-based fracture reduction in

    distal radius fracture (colles). *Journal of Emergencies, Trauma, and Shock*, *16(2)*, 35–42.

    https://doi.org/10.4103/jets.jets_157_22

Olson, N., Griggs, J., Balhara, K. S., Kann, K., April, M. D., & Olson, A. S. (2022). Evaluation
of a hands-on wrist fracture simulator for fracture management training in emergency
medicine residents. *Cureus*. https://doi.org/10.7759/cureus.27030

ORTHOfilms. (2015). *Closed Reduction of a Distal Radius Fracture*. *YouTube*. Retrieved from
https://www.youtube.com/watch?v=cy6f7he2e4w.

Pidgeon, T. S. (2022, January). *Distal radius fractures (broken wrist) - orthoinfo - aaos*.
OrthoInfo.
https://orthoinfo.aaos.org/en/diseases--conditions/distal-radius-fractures-broken-wrist/

Powell, A. R., Srinivasan, S., Green, G., Kim, J., & Zopf, D. A. (2019). Computer-Aided Design,
3-D–Printed Manufacturing, and Expert Validation of a High-fidelity Facial Flap Surgical
Simulator. JAMA Facial Plastic Surgery, 21(4), 327–331.
https://doi.org/10.1001/jamafacial.2019.0050

Raeker-Jordan, E. A., Martinez, M., Aziz, K. T., Miles, M. R., Means, K. R., LaPorte, D. M.,
Giladi, A. M., & Shimada, K. (2021). High-fidelity wrist fracture phantom as a training
tool to develop competency in orthopaedic surgical trainees. *JAAOS: Global Research
and Reviews*, *5*(5). https://doi.org/10.5435/jaaosglobal-d-20-00224

Rundgren, J., Bojan, A., Mellstrand Navarro, C., & Enocson, A. (2020). Epidemiology,
classification, treatment and mortality of distal radius fractures in adults: An
observational study of 23,394 fractures from the National Swedish Fracture Register.
BMC Musculoskeletal Disorders, *21*(1). https://doi.org/10.1186/s12891-020-3097-8

Sales, T. (2021, November 29). *Trauma training: Bone models provide hands-on learning*. Best

    Anatomical Medical Training Models Company.

    https://www.sawbones.com/blog/post/trauma-training-bone-models-provide-hands-on-lea

    rning-sb

Solgaard, S. (1985). Classification of distal radius fractures. *Acta Orthopaedica Scandinavica*,

    56(3), 249–252. https://doi.org/10.3109/17453678508993006

Søsborg-Würtz, H., Corap Gellert, S., Ladeby Erichsen, J., & Viberg, B. (2018). Closed

    reduction of distal radius fractures: A systematic review and meta-analysis. *EFORT Open*

    Reviews, *3*(4), 114–120. https://doi.org/10.1302/2058-5241.3.170063

Vescio, A., Testa, G., Sapienza, M., Caldaci, A., Montemagno, M., Andreacchio, A., Canavese,

    F., & Pavone, V. (2022). Is obesity a risk factor for loss of reduction in children with

    distal radius fractures treated conservatively? *Children*, *9*(3), 425.

    https://doi.org/10.3390/children9030425

Wrist anatomy. HandSport Surgery Institute. (2020, February 7).

    https://handsurgeonsnyc.com/patient-education/wrist-anatomy/

ÖZDEMİR, E., ALTUN, O., ERGİŞİ, Y., DAŞAR, U., & YALÇIN, M. N. (2023). The role of

    wrist circumference (regional obesity versus local swelling) in conservatively treated

    distal radius fractures: A single center experience. *Batı Karadeniz Tıp Dergisi*, *7*(1),
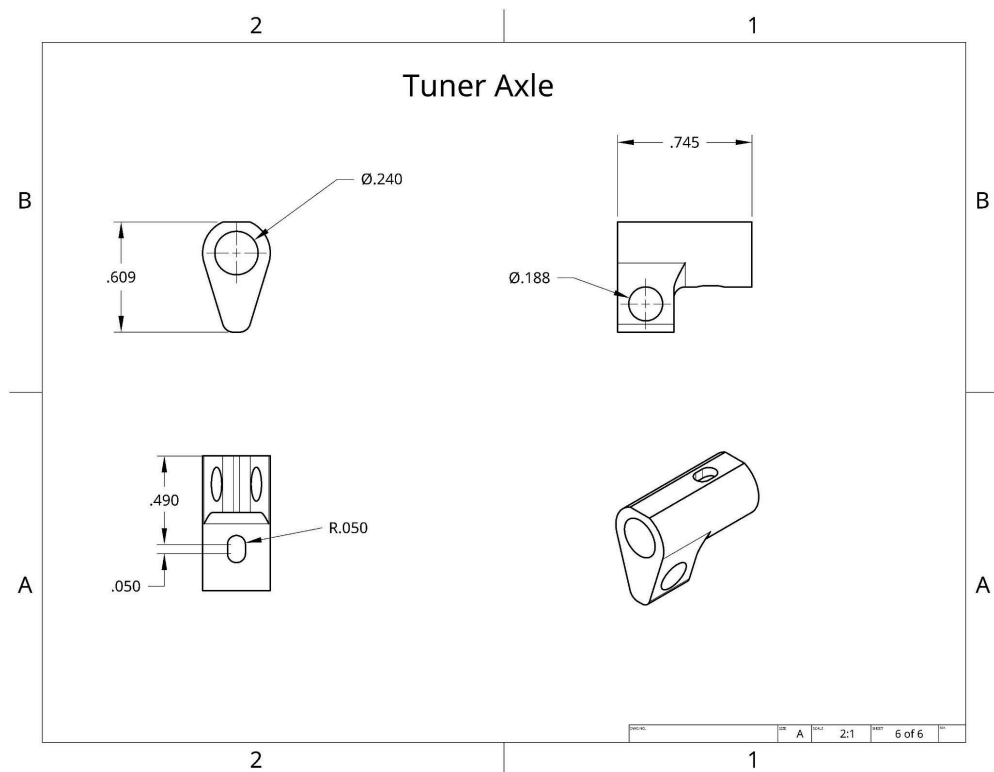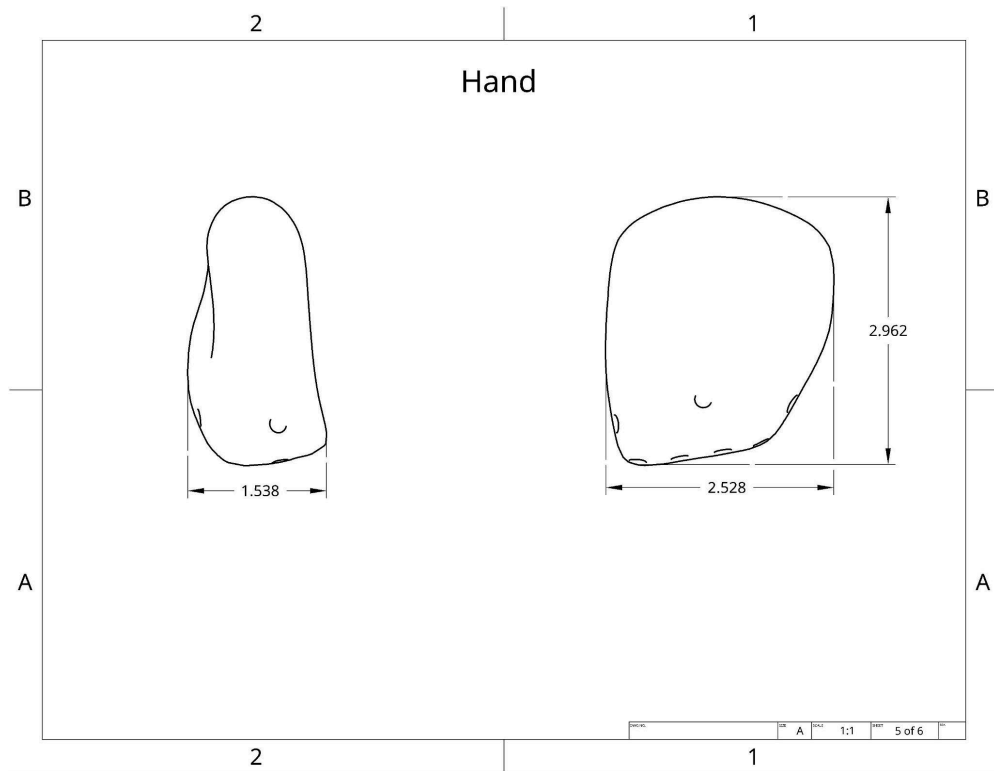
    75–80. https://doi.org/10.29058/mjwbs.1232968

Detailed Drawings

Part No.	QTY	Name	Material
1	1	Base	PLA
2	1	Radius and Ulna	PLA
3	1	Fracture Piece	PLA
4	1	Hand	PLA
5	2	Right Hand Tuner	Steel
6	2	Left Hand Tuner	Steel
7	4	Tuner Axle	PLA

14.018

2.250

7.750

UNLESS OTHERWISE SPECIFIED,
DIMENSIONS ARE IN INCHES
.XX = ±.0-
.XXX = ±.00   ANGULAR = ±°
.XXXX = ±.000   FRACTIONAL = ±
SURFACE FINISH
DO NOT SCALE DRAWING
BREAK ALL SHARP EDGES AND
REMOVE BURRS
THIRD ANGLE PROJECTION

DRAWN — RYAN DELDACH — 05/10/2025
CHECKED
APPROVED

TITLE

**Wrist Fracture Reduction
Simulator**

SIZE **A**   DWG NO.

SCALE 1:4   SHEET 1 of 6

Base

2.250

.500

1.250

.750

R.100

Ø.390x2

3.375

70.3°   1.750

7.750

1.875

Ø.201x2

1.875

Ø.188x14

SIZE **A**   SCALE 1:2   SHEET 2 of 6

Ulna and Radius

1.405

7.805

1.570

Ø.159x2

Fracture Piece

1.005

1.195

Hand

2.962

1.538

2.528

Tuner Axle

Ø.240

.745

.609

Ø.188

.490

R.050

.050

Table A1

Bill of Materials - Cost per model

Part Number	Part Name	Quantity	Cost
1	Base	1	$1.73
2	Radius & Ulna	1	$0.53
3	Fracture	1	$0.06
4	Hand	1	$0.82
5	Guitar Tuners	4	$1.77
6	Guitar Peg Covers	4	$0.03
7	Tuner Screws	4	$0.02
8	Tuner Nut	4	$0.01
9	Bone Screws	2	$0.18
10	Elastic (Fracture) (14")	4	$0.15 (14in)
11	Elastic (Hand) (8")	1	$0.09 (8in)
12	Zip Ties	4	$0.02
13	Silicone	Variable	$11.66
14	Silicone Primer	Variable	$3.52
15	Silicone Mold Side 1	1	$4.19
16	Silicone Mold Side 2	1	$4.24
17	Silicone Mold Insert	1	$1.82
18	Clamps	2	$5.99
19	Mold Screws	6	$0.18

Total cost per model: $50.08

Table A2

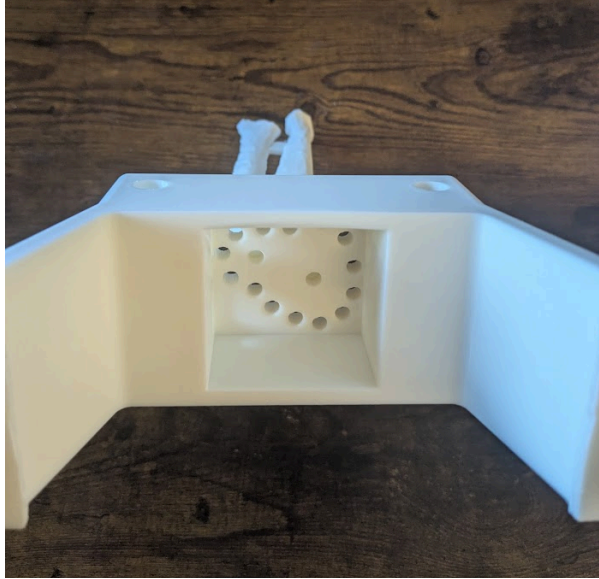Bill of Materials with Material Order Purchase Costs and Links - Total production cost
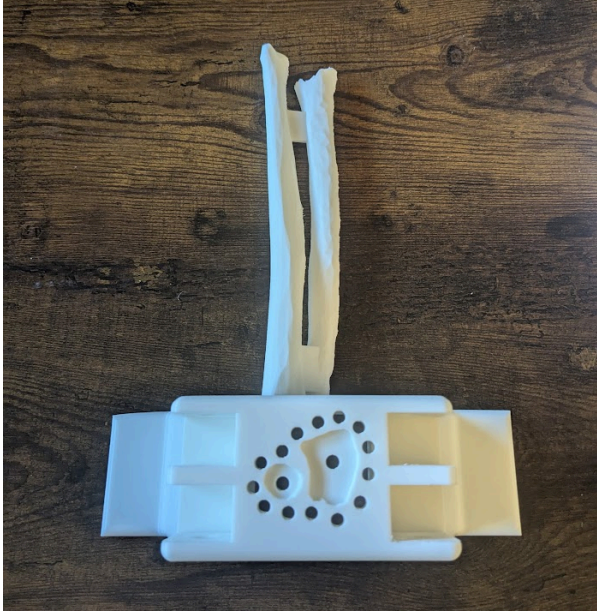
Part Number	Part Name	Quantity	Total Cost	Link
1	Base	1	$1.73	3D Print
2	Radius & Ulna	1	$0.53	3D Print
3	Fracture	1	$0.06	3D Print
4	Hand	1	$0.82	3D Print
5	Guitar Tuners	4	$10.59	Tuners
6	Guitar Peg Covers	4	$0.03	3D Print
7	Tuner Screws	4	$8.99	Screws and Nuts
8	Tuner Nut	4	Included in Above	See Above
9	Bone Screws	2	$0.36	Bought at Store
10	Elastic (Fracture)	4	$6.85	Elastic
11	Elastic (Hand)	1	Included in Above	See Above
12	Zip Ties	4	$5.99	Zip Ties
13	Silicone	Variable	$34.97	Silicone
14	Silicone Primer	Variable	$35.15	Silicone Primer
15	Silicone Mold Side 1	1	$4.19	3D Print
16	Silicone Mold Side 2	1	$4.24	3D Print
17	Silicone Mold Insert	1	$1.82	3D Print

18	Clamps	2	$11.98	Clamps
19	Mold Screws	6	$0.18	Bought at Store

Total Cost: $128.48

Instruction Manual of Assembly

Table A3:
Overview of Assembly Process

Step 1.) Gather the base and the fractured bones	**Step 2.)** Place the bones in the indented slot on the top of the base and screw them with wood screws using the bottom 2 center holes
Step 3.) Cut 4 elastic strands of equal length (14 inches) and burn the ends with a lighter so that they do not fray. Tie a plain knot on one end of all of them.	**Step 5.)** Slide the strand through the 4 holes on the sides of the fracture fragment. The knots should be at the top of the fracture piece (trim the excess string if necessary) to make it look like the image to the right.

| **Step 6.)** Pull the knots away from the fracture piece slightly, making room for the future steps | **Step 7.)** Slide a zip tie through one side hole on the flatter edge of the fracture piece, out the middle, and then back down and through the other side as shown below: |

| **Step 8.)** The piece should look like this afterwards. (In future steps, the ziptie may not be shown to lessen the clutter in the example photos; however, keep the ziptie on the | **Step 9.)** Cut and burn another strand of approximately 6 inches. |
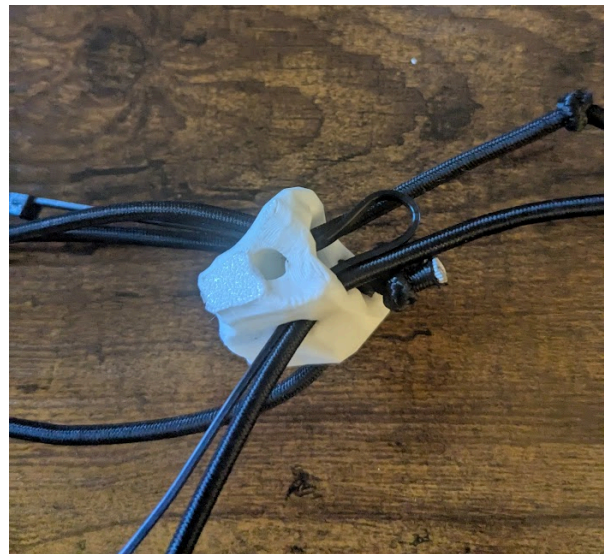
model, as it will be used later)

Step 8.) Thread the new piece of elastic through the hand piece, leaving the ends slightly uneven as shown to the right (in the image, the hand is placed concave side down)

Step 9.) Now, with the room created on the fracture piece from pulling the elastic out slightly, slide the long end of the hand elastic through the left side hole (should be larger than the right side hole) of the fracture piece.

Step 10.) Continue threading the long side of the elastic through the right hole of the ulna.

Step 11.) Tie a knot. The knot should be pulled so that it is completely tight, but it should not take much effort to tie.

Step 12.) Gather 2 right-side tuners and 2 left-side tuners and place them in all four corners with the tuner portion facing outwards and the mounting hole towards the top of the base.

Step 13.) Now that you've got them positioned correctly, put on the axles. To do this, slide the tuner out of its hole, insert the axle with the small pin hole in the inside wall of the base, and then rotate it perpendicular to the wall before sliding the tuner through the axle.

Step 14.) Repeat this for all 4 corners so the model looks as follows. Then align the hole on the axle with the hole in the tuner.


Step 15.) Decide whether to secure the axles to the tuners with the nuts and bolts listed in the bill of materials or make cotter pins out of paper clips. To make the pins bend the paper clip into the pattern below with pliers, then cut the pin off.
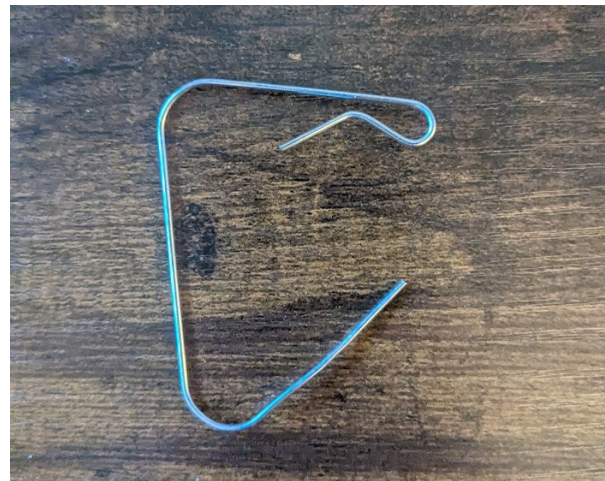
Step 16.) Insert either the pin or the nut and bolt all the way through the axle, attaching it to the tuner such that they move together
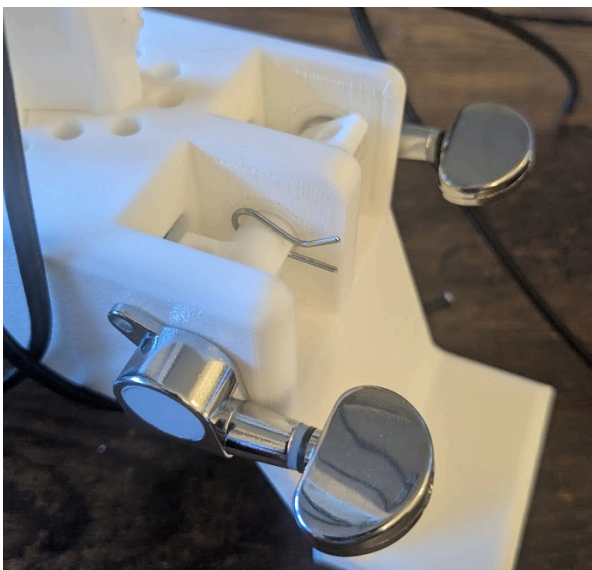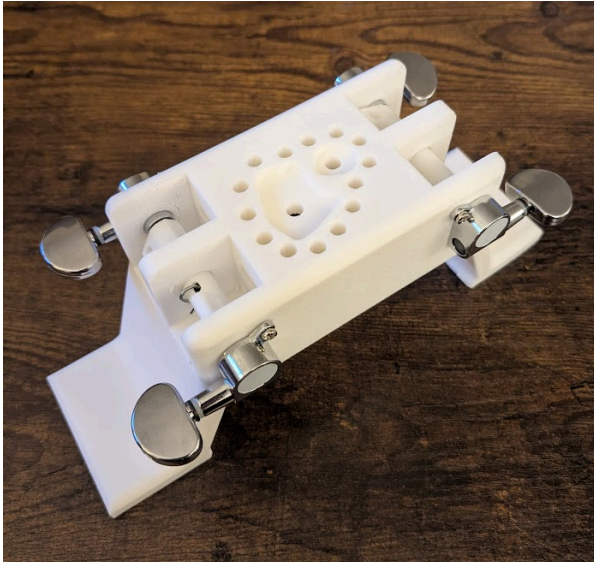

Step 17.) Ensure that the bottom of the tuner is parallel to the bottom of the base and then use a screwdriver and pressure to thread the hole
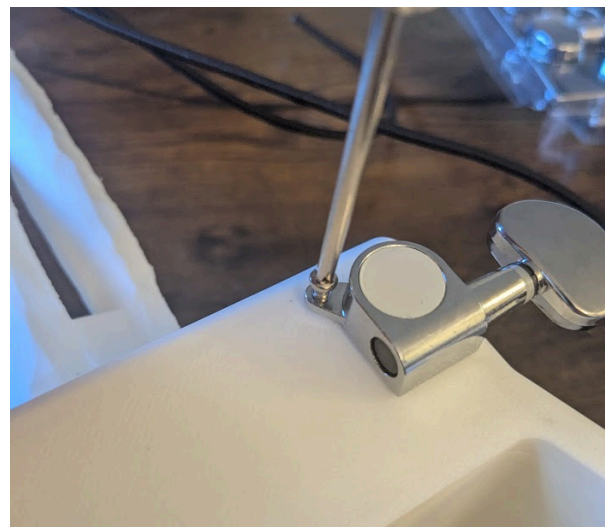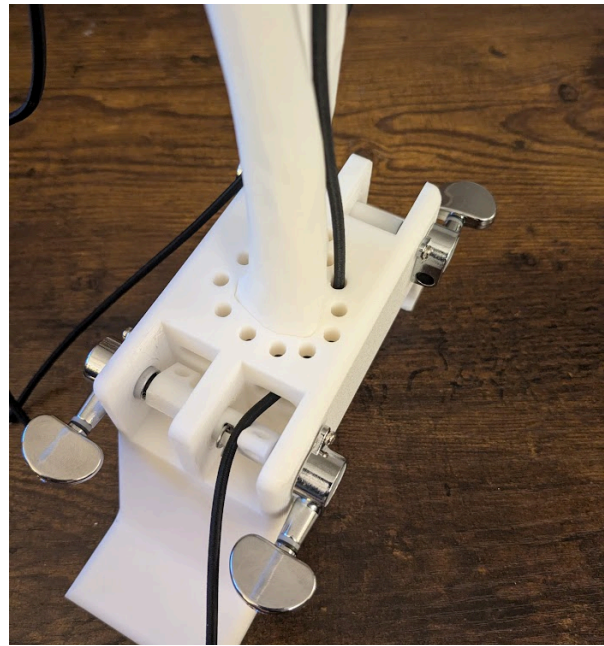

Step 18.) Repeat on all four tuners such that it resembles the image below (bones removed to

Step 19.) Thread the 4 strings attached to the fracture into the holes at the top of the base,
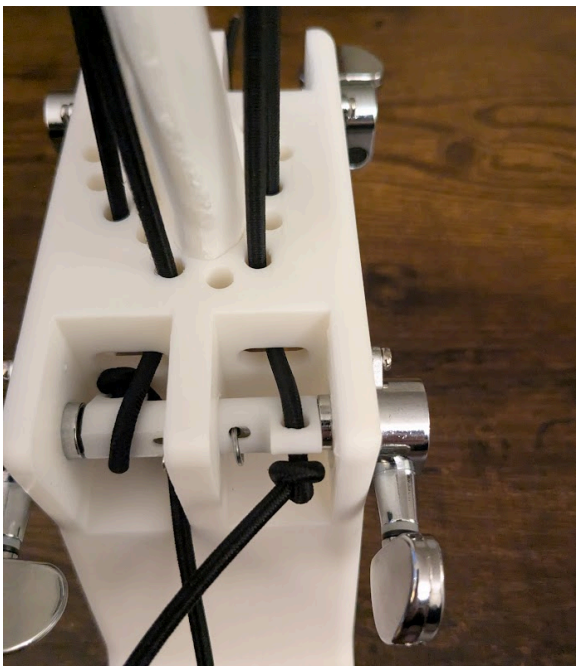
improve visibility)

out the sides, and through the holes on the axle

Step 20.) Pull the elastic taught and tie a knot on the outside of the axle, wind up all the tuners to add tension to the system
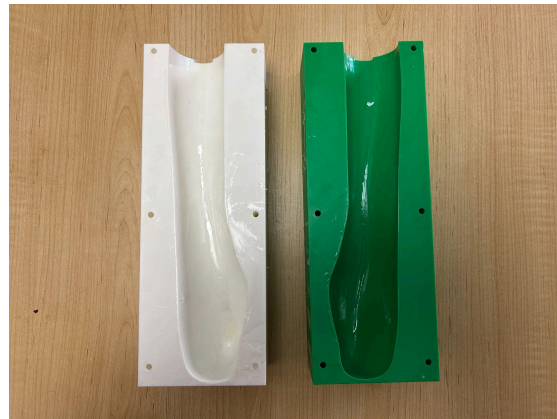

Step 21.) Now it's time to add the zip ties, take two small zip ties and thread them through the holes on the left and right side to apply a mechanical displacement limiter between the hand and the bones. The holes are shown in this image and the attached zip ties are in Step 22.
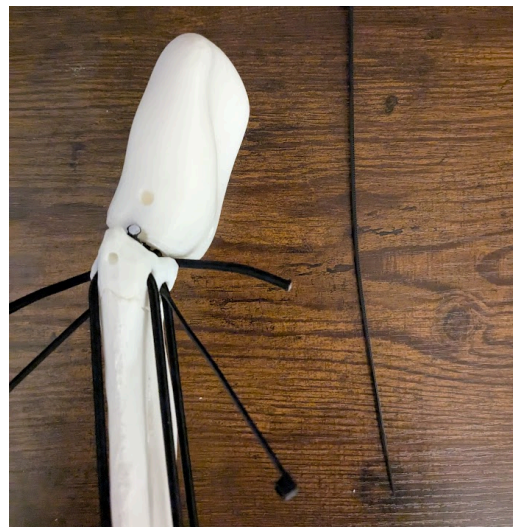
Step 22.) Tighten the zip ties on either side such that they look like the image below. Finally, thread the preplaced zip ties in the middle up through the remaining hole shown below to form a loop between the bone fragment and the hand. The tension should be similar to the other two zip ties and can be adjusted by feel. 	**Step 23.)** Mix 3-D print sealant according to the directions on the bottles. Taking the 3-D printed mold, paint sealant on all parts of the mold surface that will be touching the silicone - the inside surfaces of the outer mold along with the outside surface of the inner mold. Leave it to cure overnight, ensuring that it is smooth and not sticky to the touch before pouring silicone.
Step 24.) Put the mold together, matching the sections that say "A" together and the sections that say "B" together. Ensure that the peg on the tip of the inner mold is securely inserted into the hole on the outer mold and that there are no gaps between the mold parts, otherwise the silicone will leak out. The sides of the outer mold can be secured using long screws.	**Step 25.)** Mix the silicone according to the directions on the bottle and slowly pour into the mold, avoiding bubbles if possible. Allow to cure for at least 5 hours before removing from the mold.
Step 26.) Gently remove the silicone from the mold, being careful not to rip or snag it. If the silicone is sticky to the touch, clean the exterior with rubbing alcohol and lightly brush on a coating of cornstarch after the rubbing alcohol dries. This finishing process can be repeated if the silicone later gets sticky after use.	**Congrats on finishing the model!**